Environmental Science Advances

ROYAL SOCIETY OF CHEMISTRY

CRITICAL REVIEW

View Article Online
View Journal | View Issue

Cite this: *Environ. Sci.: Adv.*, 2023, **2**, 11

Application of neural network in metal adsorption using biomaterials (BMs): a review†

Amrita Nighojkar, ‡[a] Karl Zimmermann, [b] Mohamed Ateia, [c] Benoit Barbeau,[d] Madjid Mohseni,[b] Satheesh Krishnamurthy, [e] Fuhar Dixit ‡*[b] and Balasubramanian Kandasubramanian *[a]

With growing environmental consciousness, biomaterials (BMs) have garnered attention as sustainable materials for the adsorption of hazardous water contaminants. These BMs are engineered using surface treatments or physical alterations to enhance their adsorptive properties. The lab-scale methods generally employ a One Variable at a Time (OVAT) approach to analyze the impact of biomaterial modifications, their characteristics and other process variables such as pH, temperature, dosage, *etc.*, on the removal of metals *via* adsorption. Although implementing the adsorption procedure using BMs seems simple, the conjugate effects of adsorbent properties and process attributes implicate complex nonlinear interactions. As a result, artificial neural networks (ANN) have gained traction in the quest to understand the complex metal adsorption processes on biomaterials, with applications in environmental remediation and water reuse. This review discusses recent progress using ANN frameworks for metal adsorption using modified biomaterials. Subsequently, the paper comprehensively evaluates the development of a hybrid-ANN system to estimate isothermal, kinetic and thermodynamic parameters in multicomponent adsorption systems.

Received 23rd August 2022
Accepted 24th October 2022

DOI: 10.1039/d2va00200k

rsc.li/esadvances

Environmental significance

With growing environmental consciousness, biomaterial systems (BMS) have garnered attention as a sustainable material for the adsorption of hazardous water contaminants. These BMSs are engineered using surface treatments or physical alterations to enhance their adsorptive properties. The lab-scale methods generally employ a One Variable At a Time (OVAT) approach to analyze the impact of biomaterial modifications, their characteristics and other process variables such as pH, temperature, dosage, *etc.*, on the removal of metals *via* adsorption. Although the adsorption procedure using BMSs seems simple in implementation, the conjugate effects of adsorbent properties and process attributes implicate complex nonlinear interactions. As a result, Artificial Neural Network (ANN) have gained traction on the quest to understand the complex metal adsorption processes on biomaterials, with applications in environmental remediation and water reuse.

1. Introduction

Growing population, urbanization, and changing climate cycles stress water resources and public water supplies. The United Nations reported that 2.3 billion people live in water-scarce zones worldwide.[1] Public health and economic tensions from water scarcity will be exacerbated in regions with water tainted with metal contaminants. Such water-scarce areas deserve and need solutions to remove metal contaminants and enable water remediation and reuse.[2]

The literature has proposed physicochemical technologies like reverse osmosis, ion exchange, electrodialysis and adsorption to eliminate metallic ions from water resources and industrial effluents.[3–14] Among these technologies, adsorption is the best-suited method for treating water and wastewater due to its high efficiency with low economics.[15–23] The selection and fabrication of sustainable adsorbents for the eradication of water pollutants include the following criteria: (1) it should be inexpensive and (2) simple to synthesize in large quantities, (3) it should demonstrate high adsorption capacity and most importantly, (4) it should cause no harm to the environment. Nature-inspired biomaterials have gained attention as decontamination media owing to their non-toxic, biodegradable, and inexpensive features.[24–30] Further, many biomaterials exhibit chemical stability and structural integrity throughout repeated

[a]*Nano Surface Texturing Lab, Department of Metallurgical and Materials Engineering, Defence Institute of Advanced Technology (DU), Pune, India. E-mail: meetkbs@gmail.com*
[b]*Department of Chemical and Biological Engineering, University of British Columbia, Vancouver, Canada. E-mail: fdixit@chbe.ubc.ca*
[c]*United States Environmental Protection Agency, Cincinnati, USA*
[d]*Department of Civil, Geological and Mining Engineering, Polytechnique Montreal, Quebec, Canada*
[e]*School of Engineering & Innovation, The Open University, Milton Keynes, UK*

† Electronic supplementary information (ESI) available. See DOI: https://doi.org/10.1039/d2va00200k

‡ These authors contributed equally to this work.

adsorption and desorption cycles, enabling their use for heavy metal ions removal.[31] The porous texture of biomaterials speeds up the transport of metal ions, while the presence of phenolic, carbonyl, amide and amine-containing functional groups in biomaterials facilitate metal ion adsorption through surface complexation.[32,33] In addition, biomaterial systems have been engineered using various surface functionalization and physical alterations to tailor their surface chemistry and enhance their adsorptive capacity. For instance, our research team has prepared eco-friendly cellulose beads impregnated with nano iron oxide for thorium and arsenic retrieval;[34,35] synthesized cost-effective cellulose nanofibers and functionalized with camphor soot carbon nanoparticles for uranium extraction;[36] crosslinked starch with polyvinyl alcohol for oil–water separation;[37] electrospun nano fibres for adsorption of metal ions;[38–41] developed composites from agro-wastes for removal of metal and dyes.[42] The details of distinct physical and chemical modifications of biomaterials are illustrated in Fig. S1.†

The BMs' performance is greatly affected by environmental conditions (pH, temperature), initial metal concentration, and the structure of the biomaterial. Laboratory experiments have been used to discover high-performing BMs; however, these studies are costly for time and resources. Accordingly, modelling techniques could offer time- and resource-saving efficiency in predicting the performance of BMs for full-scale application.[43,44] Mathematical models based on multiple linear or nonlinear regression (MLR, MNLR) and response surface method (RSM) have been proposed to assess the removal potential of metallic contaminants using experimental data from isotherm and kinetic studies.[45–48] The joint role of spectroscopic analysis and RSM has been applied to enumerate the adsorptive removal of zinc (Zn(II)), cobalt (Co(II)) and nickel (Ni(II)).[49] Since these adsorption systems exhibit nonlinear adsorptive behaviours, it would be inappropriate to characterize them using conventional statistical models. In this sense, the ANN learning principles are potent means to optimize the metal adsorption process on biomaterials by establishing a nonlinear relationship between independent (pH, temperature, dose, time of contact, the concentration of metal ions, biomaterial characteristics, *etc.*) and dependent variables (metal uptake capacity, % adsorption efficiency, *etc.*) for single and multi-metallic wastewater systems.[50–53]

Studies in the past stipulated the removal efficiency of metals using various artificial intelligence (AI) models. For example, Bhagat *et al.*, 2020 examined the application of distinct AI models like kernel, evolutionary, black box, fuzzy and hybrid models for optimizing heavy metal removal.[206] Rather than illustrating the mathematical concepts necessary for automation, the author highlighted treatment procedures such as flocculation, coagulation, membrane filtration, biosorption, proposed prediction models, input and output variables, and distinct metrics for comparing model performance. Alam *et al.*, 2022; Reynel-Ávila *et al.*, 2022 categorized AI technologies and reported their use in the remediation of organic and inorganic contaminants.[207,208] Whereas Yaseen *et al.*, 2021 discussed the utility of AI in simulating soil and water bodies contaminated with metals.[209] The utilization of classical adsorption models, multicomponent adsorption, sensitivity analysis, and progression in ANN frameworks were not discussed earlier in detail for evaluating kinetics, isotherms, and thermodynamic parameters of adsorption.

This review briefly explains the main biomaterial alteration processes and discusses conventional adsorption investigations in conjunction with ANN modelling. Then, we address the pre- and post-processing methods involved in constructing ANN models and show statistics of datasets considered for optimizing metal adsorption on biomaterial systems. We describe current advancements in the ANN framework for single and multi-metal adsorption process optimization and related improvements in hybridizing isotherm, kinetics, and breakthrough curves. Next, advances in thermodynamic parameter estimations are reported to understand the nature of the adsorption process. The sensitivity analysis of ANN has also been described to comprehend the relative influence of individual and group of adsorption factors on anticipated efficiency. Towards the end, the review highlights significant challenges and advancements in the field of ANN technology for metal remediation.

2. Experimental studies and dataset of metals adsorption on BMs

A given biomaterial's interaction with metal adsorbates depends on its functional groups, the engineered surface of biomaterials, pH and temperature conditions, and physical or chemical changes in the configuration that influence biomaterials' morphology, pore size distribution, and elemental compositions. However, biomaterials without modification have constraints regarding recovery and recycling. Because of their poor porosity and limited adsorption sites, pristine biomaterials exhibit low adsorption efficacy.[54]

Thus, the engineered modifications and surface alterations of the biomaterial matrix become necessary to achieve greater adsorption capacities. Research reports the conversion of natural biomaterials into beads, foams, and nanofibers to attain better pore size distribution and durability. The surface area of biomaterials has also been enhanced *via* their conversion to nanoscale structures and activated carbon.[55–62] The surface treatment of biomaterials with acids and alkalis improved their interactions with metals, which resulted in faster adsorption rates and increased uptake capacity.[63–66] The reutilization of saturated biomaterials into value-added products has been reported in detail by authors in their earlier research.[7] The experimental adsorption studies that depict various aspects of metals adsorption relevant for ANN modelling are given below:

2.1 Adsorption kinetics

Adsorption kinetics gives vital information about the associated mechanism and equilibrium time required to sequester maximum metal impurities from an aqueous solution. The period of contact (CT) between the biomaterial and metal adsorbate and equilibrium time (t_e) corresponding to specific

Table 1 Time required (t_e) to reach equilibrium for the metal adsorption process using biomaterials[a]

Metal adsorbed	Biomaterials	CT (min)	t_e (min)	C_o (mg L^{-1})	Reference
As(v)	Iron oxide permeated mesoporous rice-husk	0–1440	1440	60	63
Cd(ii)	Alkali-modified oak waste residues	0–240	60	25–100	64
Co(ii)	Alginate-SBA-15 nanocomposite	0–300	300	100	58
Cr(vi)	Nanocomposite from sawdust biochar	0–200	120	50	67
Cr(vi)	Acidically prepared rice husk carbon	0–180	120	60	68
Cr(vi)	Activated carbon from medlar seed	0–130	60	200	69
Cr(iii), Cr(vi)	Nanocrystalline cellulose	0–60	40	25	70
Cr(vi)	Iron ions doped on the rice husk	0–240	240	50	71
Cu(ii)	Banana floret	0–60	60	50	72
Cu(ii)	Orthophosphoric acid–modified biochar	0–60	60	10	73
Pb(ii)	Rice husk carbon (RHC)	0–120	120	60	74
Pb(ii)	Carboxylate-functionalized walnut shell	0–15	15	100–220	75
Pb(ii)	Rice husks digested with nitric acid	0–180	120	20–80	76
Hg(ii)	Activated carbon derived from local walnut shell	0–120	60	50	77
Ni(ii)	Alginate-based composite bead (AB)	0–100	80–100	100	59
Th(iv)	Chitosan/TiO_2 nanocomposite	0–70	70	200	78
U(vi)	Polyacrylonitrile grafted potato starch-based resin	0–120	120	20	79
U(vi)	$KMnO_4$-modified hazelnut shell activated carbon	0–200	160	100	66
Zn(ii)	Rice husks digested with nitric acid	0–120	15–90	25	65
Co(ii), Ni(ii)	Alginate nanoparticles	0–80	80	80.115, 10.523	55
Cr(vi), Cu(ii)	Wheat straw	0–60	15, 30	20	80
Cd(ii), Pb(ii), Ni(ii)	Functionalized wood pulp	0–40	40	25	81

[a] CT = contact time, t_e = equilibrium time, C_o = initial concentration of metals.

metal concentrations (C_o) are listed in Table 1. The kinetics adsorption data using modified biomaterials fitted best with the pseudo-second-order equation, where the values of kinetic model parameters differ regarding when the equilibrium time is reached. The experimentally obtained details (initial metals concentration, contact time and equilibrium time) will aid in developing ANN-driven kinetic models for predicting the significant kinetic parameters and uptake capacity detailed further in Section 5.

2.2 Adsorption isotherms

Adsorption isotherm models describe the maximum adsorption capacity at equilibrium adsorption conditions. Table 2 displays the adsorption isotherm data for modified biomaterials for different metal ions. The Langmuir isotherm best characterized the adsorbent–adsorbate interactions for biomaterials, suggesting monolayer adsorption of metal ions on the biomaterial surface. In general, the use of linear empirical models to evaluate the isotherm parameters of the nonlinear adsorption process is becoming obsolete as it does not explicitly describe the simultaneous adsorption pattern over a wide range of operating temperatures and metal ion concentration.[82] Furthermore, because most industrial wastewaters contain numerous metal pollutants, single-species models do not adequately reflect the complex propensity of multicomponent adsorption. For this purpose, the isotherm parameters evaluation using hybridizing isotherms with ANN, as discussed in Section 5, is gaining popularity.

2.3 Thermodynamics

Thermodynamic parameters offer insights into the impact of changing environmental conditions (*i.e.* temperature) on the nature of the adsorption process using modified biomaterials. Table 3 details the adsorption process's temperature range, feasibility, and nature. The data will aid in modelling thermodynamic conditions for predicting thermodynamic parameters (*e.g.*, Gibbs free energy changes) across a wide range of adsorption conditions, as discussed in Section 5.

2.4 Adsorption data set based on BMs and pre-processing

The biomaterials in the current review included cellulosic, alginate and chitosan-based biomaterials. Compared to other polysaccharides, plant and agriculture-based biomaterials have been extensively modelled for metal remediation purposes (refer to ESI, S2†). The standards for modifying the biomaterials mentioned above are found in the literature.[55,59–61,70,71,80,81,83,84] The physicochemical features of the reviewed modified biomaterial systems were determined by different analytical techniques such as BET, FTIR and SEM-EDS. The morphology of some of the modified BMSs under a scanning electron microscope is shown in Fig. S2.†

Experimental data is an essential prerequisite in processing the ANN framework. The details of the diverse dataset, including the characteristics of biomaterials, environmental conditions (temperature, pH) and process variables, are given in Section S2.† The experimental dataset contained 15 variables,

Table 2 Model parameters of the adsorption isotherm used in the adsorption of specified metal contaminants onto the listed biomaterials adsorbents

		Langmuir		Freundlich		Redlich–Peterson			Dubin–Redushkevich		
Metals adsorbed	Biomaterials	Q_{max} (Mg g^{-1})	K_L (L mg^{-1})	K_f (mg g^{-1}) (mg L^{-1})^a	$1/n$	K_r (L g^{-1})	α (L^{θ} mg^{θ})	θ	Q_m (mg g^{-1})	K_{dr} (mol^2 kJ^{-2})	References
Cd(II)	Alkali-modified oak waste residues	771.4	0.006	—	—	—	—	—	—	—	64
Co(II)	Alginate-SBA-15 nano composite	78.1	1.04	—	—	—	—	—	—	—	58
Cr(III)	Nanocrystalline cellulose	2.88, 2.77	1.49, 0.48	—	—	—	—	—	—	—	70
Cr(VI)	Acidically prepared rice husk carbon (APRHC)	47.62	0.018	—	—	—	—	—	—	—	68
Cr(VI)	Activated carbon from medlar seed	212.76	0.072	—	—	—	—	—	—	—	69
Cr(VI)	Iron ions doped on the rice husk	—	—	0.63	0.28	—	—	—	—	—	71
Cr(VI)	Chitosan foamed structure	10.08	—	—	—	—	—	—	—	—	61
Cu(II)	Orthophosphoric acid-modified biochar derived from coconut (cocos nucifera) husk	175.438	0.372	—	—	—	—	—	—	—	73
Pb(II)	Rice husk carbon (RHC)	62.5	0.23	—	—	—	—	—	—	—	74
Pb(II)	Carboxylate-functionalized walnut shell	192.31	0.36	15.27	0.43	—	—	—	—	—	75
Hg(II)	Activated carbon derived from local walnut shell	80	0.0088	—	—	—	—	—	—	—	77
Ni(II)	Alginate-based composite bead (AB)	—	—	—	—	76.45	7.98	0.82	1.539	1.262×10^{-8}	59
Th(IV)	Chitosan/TiO_2 nanocomposite	455	—	—	—	—	—	—	—	—	78
U(VI)	$KMnO_4^-$modified hazelnut shell activated carbon	22.27	0.041	—	—	—	—	—	—	—	66
Co(II), Ni(II)	Alginate nanoparticles	21.46, 6.199	0.062, 0.026	—	—	—	—	—	—	—	55
Cr(VI), Cu(II)	Wheat straw	09.19, 5.38	0.4598, 2.57	—	—	—	—	—	—	—	80
Zn(II), Cu(II), Cr(VI)	Chitosan foamed structure	5.675, 17.77, 10.8		—	—	—	—	—	—	—	61

Table 3 Details of nature of adsorption process at different temperature ranges

Metal adsorbed	Biomaterials	Temperature range (K)	Adsorption process	References
Cd(II)	Alkali-modified oak waste residues	298–313	Exothermic	64
Co(II)	Alginate-SBA-15 nanocomposite	308–328	Endothermic	58
Cr(VI)	Acidically prepared rice husk carbon	298–333	Endothermic	68
Cr(VI)	Activated carbon from medlar seed	298–318	Exothermic	69
Cr(VI)	Iron ions doped on the rice husk	293–323	Endothermic	71
Pb(II)	Rice husk carbon	298–333	Endothermic	76
Ni(II)	Alginate-based composite bead (AB)	298–358	Exothermic	59
Cu(II), Cr(VI)	Wheat straw	298–318	Exothermic	80
Cd(II), Pb(II), Ni(II)	Functionalized wood pulp	298–318	Exothermic	81
Th(IV)	Chitosan/TiO_2 nanocomposite	298–318	Endothermic	78
U(VI)	$KMnO_4^-$ modified Hazelnut shell-activated carbon	298–318	Exothermic	66

including initial concentration (C_0), pH solution (pH), temperature (T), biomaterial characteristics (surface area, particle size), contact time (CT), bed depth (BD), flow rate (FR), agitation speed (AS), the volume of solution (V), pyrolysis temperature (PT), effluent concentration (EC), medium of solution (MS), bias (B), metal pollutant efficiency (MPE%) and adsorption capacity (AC). MPE % and AC were the output variables; the remaining variables were applied as input variables. A few studies used final concentration (FC), final pH (FpH), and change in Gibbs free energy (dG) as the output variable in conjunction with MAE% and AC. The frequency of individual variables used by researchers is illustrated in Fig. S3.†

Pre-processing experimental data using Pearson's correlation matrix is carried out to analyze the relationship among adsorption variables. In the cellulose-based biomaterials, the correlation matrix showed a complex correlation between process variables.[85] However, in the case of carbon-enriched BMSs, it was worth mentioning that the oxygen to carbon ratio (O : C) and the sum of oxygen and nitrogen to carbon content (O + N : C) showed an absolute correlation.[86] Hence, one of these two variables was eliminated as they represented the same data from the database. The (O + N : C) variable had a better connection with the output variable over O : C; thus, it becomes a strong contender to increase the precision of the models and explain the characteristics of the dataset employed. As illustrated in Fig. 2, the boxplot shows the range of key variables considered for modelling metal adsorption on biomaterial systems.

Post–pre-processing, the complete dataset is taken and randomly divided at 70 : 30.[58] 70% of the data is used for training the ANN model, while 30% is used for validating and testing the performance efficiency of ANN. The distribution of the attributes (ESI, S2†) shows a skewness in data distribution which can significantly affect the stability and accuracy of the ANN predictive models. Therefore, the features of the dataset are normalized using the Minmax function.

3. ANN for modeling for metal adsorption

3.1 Layman's guide to ANN

Artificial Neural Networks are inspired from a biological brain conceptual model to solve complex problems.[87] Consider how a human brain distinguishes between different people: every human has a similar overall structure (*e.g.*, two eyes, two ears, one nose, *etc.*), yet we can recognize people easily because learnings in the brain are intuitive. Instead of learning the face structure to identify people, it discovers the deviation of the face from a reference face, for example, 'h*ow different one's nose is from the generic nose, which is then quantified as a signal with a specific strength*'. Likewise, it learns the deviations from all parts of the face from a reference base case, combines these variations into a new dimension, and finally gives an output, which is the recalled identity of the good-looking person in front of you. All these steps in the brain occur in a fraction of a second. A neural network uses a similar algorithm, but the artificial neurons process the information using a mathematical approach (Fig.S4†).

The ANN architecture is organized into 3 layers: (1) an input, (2) a hidden or intermediate layer, and (3) an output layer. The information is first received by neurons in the input layer, then passed on to a set of neurons associated with single or multiple hidden layers. The job of a hidden layer is to process the information coming from input neurons using weighted connection and activation functions to calculate the output of a neuron. The data is processed from one neuron to the other, similar to the deviations learned by the human brain. The greater the outcome of a neuron, the greater would be the influence of that input dimension. These attributes are combined in the next layer using mathematical formulations to form additional new details. When multiplied several times, this procedure develops a complex network with several connections.

The neural network learns through intuitive wisdom with the help of a learning or training mechanism. For a given set of input data, the output layer makes predictions by applying a matrix multiplication series that could be either accurate or inaccurate. Based on the output, the learning mechanism gives feedback for improving the prediction efficiency of the network. The system uses a backpropagation algorithm as a feedback mechanism to incrementally update the randomly initialized weights applied to the input data for correct predictions.[88]

3.2 Generation of the ANN model

Fig. 2 illustrates the flow chart for modelling the metal adsorption process *via* ANNs. Initially, the experimental

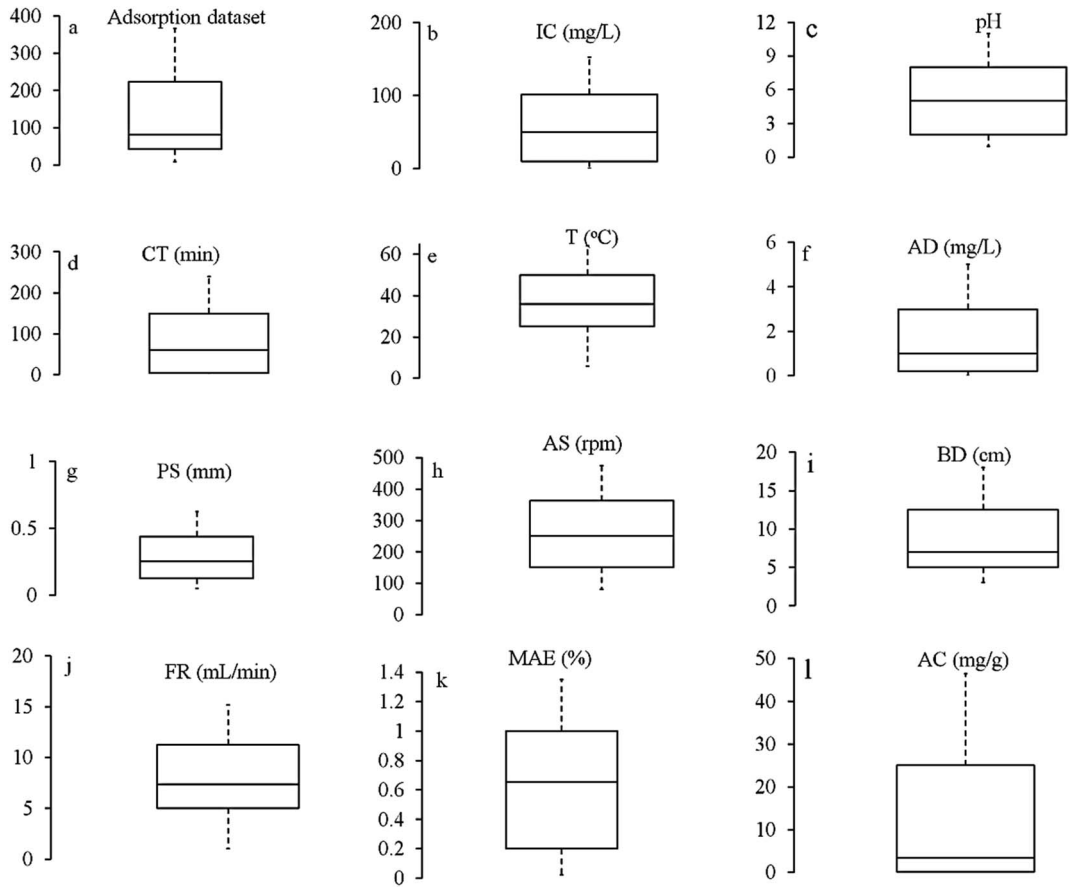

Fig. 1 The dataset before analyzing and processing (the box plots generated using data listed in ESI, Tables S1 and S2†) *AD = adsorbent dose, IC = initial concentration, CT = contact time, T = temperature, PS = particle size, BD = bed depth, FR = flow rate, AS = agitation speed, MPE = metal pollutant efficiency, AC = adsorption capacity. *The middle line in the box represents the median, the center line represents the mean, while the bottom and top lines of the box represent the 1st and the 3rd quartiles, respectively.

adsorption variables containing independent and dependent parameters are collected from lab experiments compiled from the literature. The acquired database is generally divided into training, validation, and test sets. Since the adsorption data of metal ions constitute many features (as shown in Fig. 1), the associated hyperparameters of neural network function also increase, raising the model's complexity. In such scenarios, a larger proportion of data (~70%) is kept in the training subset to make the model learn the patterns of the data, while the rest 30% of data is used for validating and testing the model performance. The network is trained to find the optimal combinations of intermediate neurons and interior layers that minimize the prediction error or loss. The neural network is trained using backpropagation (BP) algorithms which consist of the following steps, corresponding to the steps listed in Fig. 2:

(1) Selection of training data from the experimental data set.

(2) Identification and division of input and output variables.

(3) Forward propagation: it takes a weighted sum of inputs (by multiplying each input variable with an assigned weight) and bias. This weighted output is then passed through an activation or transfer function, which introduces nonlinearity into the result. (For mathematical interpretation, refer to ESI, S.2.2†). Depending on the activation function used, the outputs are normalized between either 0 and 1, −1 to +1, or 0.1 to 0.9. Table S3† lists activation functions applied for the nonlinear transformation of adsorption data.

(4) Backpropagation: the ANN calculates the difference in error between the experimental observation and the expected model output using the gradient descent method. When the error exceeds the acceptable value, the weights are adjusted by multiplying the error by the input and the transfer function's gradient (*e.g.*, *tansig* function, which is the most common) (ESI, S.2.2†).

(5) Optimization is achieved by reducing the error between observed and model-predicted responses by varying neurons in hidden layers, transfer functions, training algorithms and iterative modification of weights assigned to links emerging from the input layer.[87,89] Steps 5 and 6 (of Fig. 2) are repeated until further weight changes do not reduce errors (refer to S5.2†).

(6) The performance of the ANN for modelling adsorption is evaluated using different statistical indices (Fig. 2 step 7, 8). The researchers most commonly used the coefficient of determination (R^2) and correlation coefficient (R) as efficiency evaluators, whereas Root Mean Square Error (RMSE) and Mean Square Error (MSE) are used for evaluating modelling error. The mathematical formulations of these four statistical parameters are given in S5.3.†

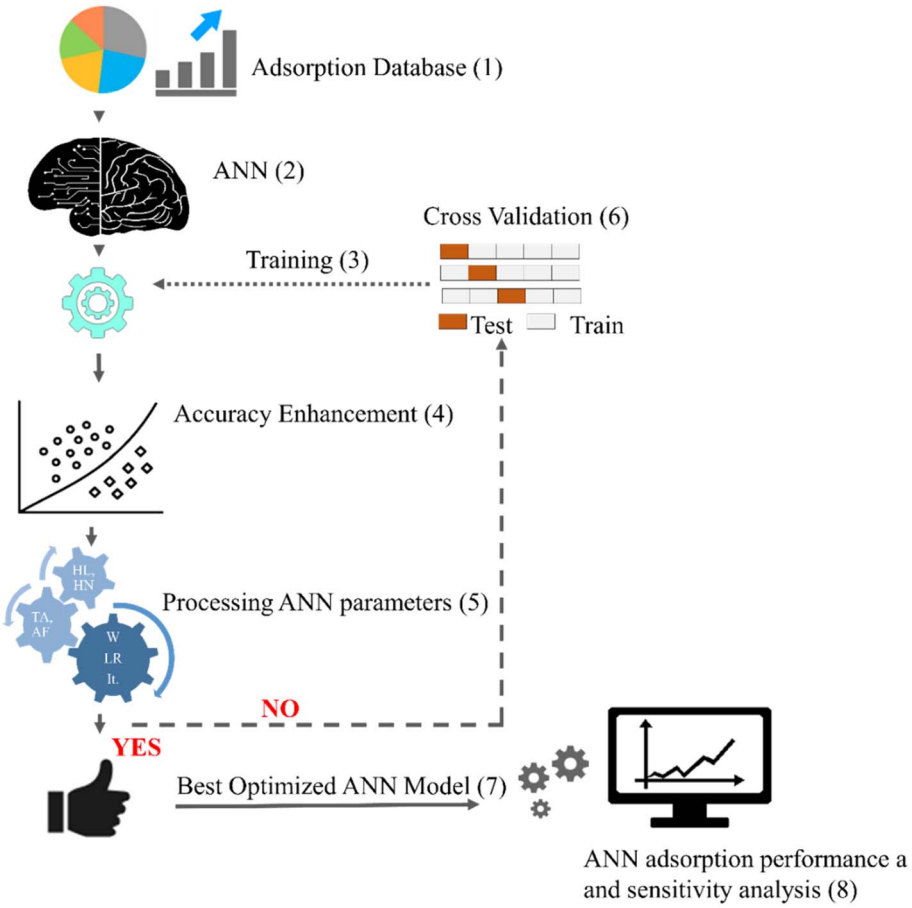

Fig. 2 Standalone ANN-framework for predicting metal adsorption onto biomaterials.

The illustration of the feedforward neural network (FFNN) that modelled the adsorption of the metal on biomaterials is presented in Fig. S5.†

4. Progressions in ANN frameworks for optimizing metal adsorption process using BMs

4.1 Standalone ANN frameworks

The purpose of the optimization is to achieve the maximum metal removal efficiency and uptake capacity of biomaterials used to recover metals and other contaminants from industrial wastewater for environmental protection and water purification. The optimization pathways reported in the literature are a compilation of variables influencing the design of adsorption systems and the adsorption process.[90] The variables affecting the adsorbent modification or preparation conditions and the metal adsorption efficacy include biomaterial dose, surface type and thermal treatments. Under the batch adsorption systems, the adsorption attributes that affect the process behaviour include the initial concentration of metal pollutants, pH of the aqueous solution, volume and medium of adsorbate solution, agitation or shaker speed, temperature and contact time. In continuous column set-up, metal concentrations, bed depth and flow rate are of primary concern (Table S4†). Some studies also included the influence of lingo-cellulosic functional groups, particle size, and calcination temperature used to optimise biomaterial adsorbents' fabrication.[52,65,66,91,92] Table 4 illustrates recent developments of ANN-based optimization methods for modelling biomaterial adsorption systems.

s described in Section 3.2, the ANN framework has been extensively implemented to optimize the variables mentioned above to attain conditions for the maximum metal adsorption efficiency or metal adsorption capacity. The details of optimal ANN architecture, activation function and modelling error corresponding to each study are depicted in Table S5.† It is to be noted that the ANN training parameters such as epoch size, learning rate, momentum and gradient influence the optimal feedforward architecture. The data division in training, validation and testing subsets and information on maximum epochs (iterations) used is illustrated in Fig. 3 (taken from Table S5–S7†).

Table 4 lists the recent developments in ANN frameworks for simulating metal adsorption on biomaterials. While back-propagation (BP) algorithms are prominently reported in the literature for the optimization of various adsorption variables, algorithms based on experimental designs such as the Taguchi method which use orthogonal arrays to identify critical

Table 4 Recently applied optimization methods in adsorptive removal of metals using biomaterials

Metal Pollutant	Biomaterial	Method of optimization	Model error (RMSE)	Reference
Cd(II),Al(III), Co(II), Cu(II), Fe(III), Pb(II)	Chitosan and chitosan-montmorillonite nanocomposite	ANN-SOS	$R = 0.96$	83
Pb(II)	Hydroxyapatite/chitosan nanocomposite	ANFIS	$R = 0.98$	60
Pb(II), Co(II)	Rafsanjan pistachio shell	ANN-GWO	1.12	101
As(V)	$ZnCl_2$ activated carbon enriched biomaterial from *Opuntia ficus indica* biomass	Hybrid-ANN isotherms and kinetics	$R^2 = 0.99$	102
Pb(II)	Iron oxide nanocomposites from bio-waste mass	ANN	0.000076	85
Cr(VI)	Alginate immobilized *Sargassum* sp.	ANN-GA[a], ANN-SA, Taguchi design	0.07[a]	93
Cu(II), Pb(II), Zn(II), As(III), Cd(II), and Ni(II)	Carbon enriched biomaterial	ANN-QSS	0.074	103

[a] Least error from ANN-GA.

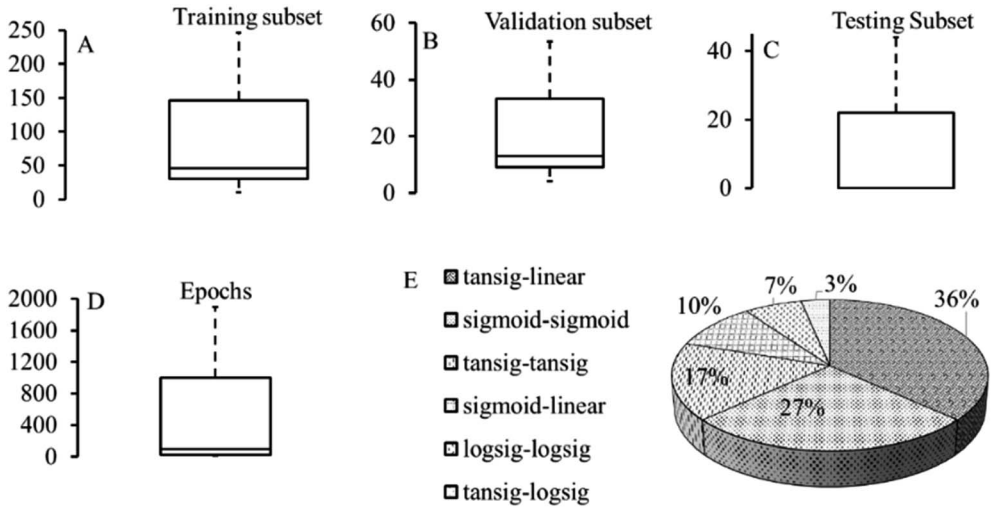

Fig. 3 Dataset, maximum epoch size and activation functions considered for ANN model development with step size = 0.01, momentum = 0.7–1, minimum gradient = 0.062. (The graphs were generated using data from ESI, Section S5†).

variables that can affect the adsorption process.[93] Algorithms based on 2-level factorial design (FFD) have also been employed with ANN to reduce the burden of laboratory experiments and determine the optimum process variables that can maximize metal adsorption on the biomaterials. For example, Popoola, 2019 used 2^k FFD to evaluate the optimal preparation condition of carbon-enriched biomaterial that can boost cadmium removal efficiency.[94] The authors used magnetite loading, walnut shell: rice husk ratio, calcination temperature and time as variables to conduct $2^4 = 16$ *i.e.* 16 sets of experiments. It was observed that a small set of experiments were sufficient to predict the optimal adsorbent conditions (*i.e.* carbonaceous biomaterial calcinated at 1000 °C for 5 hours and loaded with 10 wt% magnetite coating) that will yield maximum cadmium removal (~97%) from aqueous solution.

The RSM has been employed to conceptualize the interaction effects among independent adsorption variables.[95] RSM uses the Box–Behnken Design (BBD) to investigate the interactions between different adsorption variables, for example, initial metal concentration, pH and biomaterial dose. The BBD works as a second-order polynomial equation. Following the solution of the BBD model, the analysis of variance (ANOVA) and regression coefficients of the whole polynomial model is used to evaluate the contribution of each process variable individually and collectively.[47,63,96–98]

The RSM approach is only confined to a quadratic equation; thus ANN-based model offers broader competence to capture the complex and nonlinear behaviour of the metal adsorption process from effluents with a wide spectrum of dependent factors.[57,75,86,99,100] While ANN models for metal remediation call for advanced computing abilities, Narayana *et al.*, 2021 proposed an ANN-based graphical user interface (GUI) for experimentalists or researchers unfamiliar with computation to extract adsorption data for a particular dataset.[85]

4.2 Ensemble ANN frameworks

The standalone ANN framework trains the adsorption data using the backpropagation (BP) training algorithm. Given that BP uses the gradient descent approach to update the network's

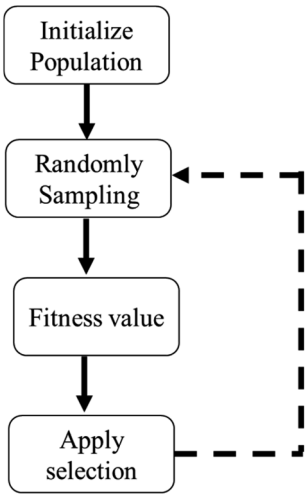

Fig. 4 A general working scheme of a metaheuristic algorithm.

link weights, the network may converge prematurely or get stuck in local minima.[104,105] Because of such drawbacks, ANNs can fall short of expected performance. To overcome such problems, ANN is bagged with metaheuristic algorithms for efficient optimization.[106–109] The flow chart illustrating any metaheuristic system's general framework is given in Fig. 4.

Hamidian *et al.*, 2019 used the Symbiotic Organisms Search (SOS) algorithm in conjunction with ANN to optimize heavy metals removal (Fe(II)), Cu(II), Co(II), Cd(II) and Al(III)) using chitosan-based nanomaterials.[83] The authors applied adsorbent dose, pH and initial concentration of metals as input parameters to the network. The symbiotic search algorithm (SOS) is a recently developed algorithm based on SI (Swarm Intelligence) that simulates the cooperative behaviour observed in nature among individuals. It generates a new solution using three coexisting behaviour types between paired organisms in an ecosystem: mutualism, commensalism, and parasitism. Mutualism is an interaction between two species with mutual benefit, meaning both benefit from the relationship. Commensalism occurs when one species forms a bond with another, and one species benefits while the other is unaffected. When two species form a relationship in which one benefits and the other hurts, it is referred to as parasitism. Both mutualism and commensalism focus on creating new species for the next generation. The parasitic phase prevents the search process from escaping the local minima. The ANN-SOS framework is illustrated in Fig.S6.†). The integration of ANN with SOS predicted metal removal efficiencies with $R^2 > 0.9$ in short computation time (50 runs) and fast convergence (<20). The SOS has drawn considerable attention in several optimization fields as compared to differential evolution (DE) and particle swarm optimization (PSO) due to its simple procedure and consistency in accurate predictions.[110–113]

Moradi *et al.*, 2020 used a hybrid of Bayesian regularization (BR) and Grey wolf optimizer (GWO) with ANN to model Pb(II) and Co(II) adsorption on pistachio shells.[101] The ANN space was initially optimized using the BR algorithm, using principles of probability distributions to prevent overfitting of the ANN. The three input parameters, *i.e.* temperature, adsorbent dose and initial concentration of metals, were then further optimized by applying GWO to the space of BR-ANN for maximum metal ions removal. The GWO is a new global optimization approach that simulates grey wolf leadership and natural hunting.[114] In GWO's hierarchy, the alpha is considered the group's dominant agent (best solution). The next subordinate to alpha includes beta (second fittest solution) and delta (third fittest solution), and omega wolf denotes the weakest solution. Additionally, three main phases of hunting, *i.e.* search for prey, encircle the prey and attack', have been implemented for optimization. The framework of BR-ANN-GWO is shown in Fig. S7.† The ANN-BR-GWO framework predicted the metal adsorption with considerably improved accuracy ($R^2 = 0.99$, RMSE = 1.1) against ANN-GWO ($R^2 = 0.96$, RMSE ~2.2. GWO's robust search capability prevents the algorithm from getting trapped in a local optimum. In GWO, achieving the right balance between the ability to explore and exploit is easy, so it can effectively solve many complex problems when coupled with ANN.[115] ANN-GWO has also been successfully used to predict the performance of desalination plants and crop yields,[116] to globally predict COVID-19 disease,[117] measure pan evaporation to compare irrigation water needs[118] and to prevent cyberattacks in our networks.[119]

Prabhu *et al.*, 2021 successfully used a Genetic algorithm (GA) to determine the recovery of chromium from alginate immobilized Sargassum in a fixed bed column. GA works on the principles of Darwinian biological evolution from natural selection, where individuals are chosen from the population to serve as parents, after which they are employed to bear the future generation's offspring.[93] The population "evolves" to the best option through future generations. In Fig. S9,† the ANN-GA framework is displayed. In their study, the authors tuned the chromium concentration, bed length and flow rate to maximize the adsorption of chromium metal. ANN-GA showed better productivity (RMSE = 0.07) against Boltzmann statistical thermodynamics (Simulating Annealing (SA), RMSE = 0.8) (van Laarhoven & Aarts, 1987). The development response of ANN-GA for predicting metals adsorption showed a better statistical quality compared to traditional statistical models.[45,78,210] The ability of evolutionary GA to address any optimization problems by tuning the selection mechanism and varying the values of genetic operators as per the problem makes these techniques superior to classic numerical optimizations. GA-ANN has attracted significant attention due to its multiple advantages (*i.e.* simple method, robust response to changing conditions and flexibility *etc.*) in solving real-world problems. These include predicting energy consumption in buildings,[120] detecting fatal heart disease,[121] solving hydrogeology problems[122] and optimizing machine parameters to reduce surface roughness[123] *etc.* The ability of GA to incorporate domain-specific knowledge into the algorithm results in a more efficient exploration of the state space of possible solutions.

Further, the two-step method for self-adapting parameters that govern evolutionary search relieves the human operator from the requirement to manually create solutions, which either consumes time or it is difficult.[124] Evolutionary algorithms can be hybridized with other models to address particular real-world problems.[125]

More recently, Zheng and Nguyen, 2022 have implemented Queuing Search Algorithm (QSA) to update the weights of ANN using the three main activities of humans in queuing: (i) prefer following the customer queue with prompt service. (ii) Effect of customers or employees on customer service. (iii) Impact of not maintaining the queue on customer service.[103] The QSA model stimulates the queening system, as described in ref. 126, to optimize the adsorption of metals, *i.e.* arsenic (As(II)), cadmium (Cd(II)), nickel (Ni(II)), copper (Cu(II)), lead (Pb(II)) and zinc (Zn(II)) on carbon-enriched biomaterial. The model used initial concentration, total carbon content, pH of the solution and pyrolysis temperature as input and metals adsorption efficiency as the output. The details of the ANN-QSA optimization procedure is illustrated in Fig.S10.† The adsorption efficiency predicted by the ANN-QSA model was closer to the metal adsorption efficiency of metals (*i.e.* RMSE = 0.051 and RMSE = 0.074 for the training and testing datasets, respectively). The standalone ANN model predicts adsorption efficiency (*i.e.* RMSE = 0.076 and RMSE = 0.097 for the training and testing datasets, respectively). The QSAs have been used to optimize mechanical design problems (*e.g.* spur gear drive systems),[127,128] but its hybridization with ANN has been reported first time for wastewater treatment applications.

Besides combining metaheuristic algorithms with ANN, a fuzzy model has been coupled with ANN to capture the nonlinearity of the metal adsorption process. The ANFIS structure consists of five layers with two types of nodes: fixed and adaptable (details, refer to S5.9.3†). Nodes in the membership function layer and the next layer are tuneable, while the rest nodes are fixed. The neuro-fuzzy arrangement uses ANN learning principles and logical reasoning to map input parameters through membership functions to generate output(s). The details of ANFIS architecture can be seen in S5.9.3.1† Sadeghizadeh *et al.*, 2019 integrated a fuzzy system with ANN to predict Pb(II) adsorption on hydroxyapatite/chitosan nanocomposite.[60] The authors considered hydroxyapatite (Hap) concentration, temperature, time, pH, agitation speed, adsorbent dose and initial Pb(II) concentration as input model parameters and lead removal efficiency as model output response. ANFIS models the Pb adsorption process by combining fuzzy "if-then" logic with neural networks' superior learning capabilities (II). The anticipated model outcomes and the experimental findings were remarkably consistent, with a correlation coefficient (R) close to unity and negligible model error. The ANFIS modelling results for metals remediation using various biomaterials have outperformed results obtained using standalone ANN frameworks and conventional statistical models.[52,84,91,129] Despite its acceptance in many other fields, including, *e.g.* medicine,[130] energy,[131] sports[132] and passenger demand forecasting,[133] ANFIS suffers from the curse of dimensionality and computational cost. The complicated structure and gradient learning in ANFIS add to the computation cost of ANFIS.

4.3 Assessment of conventional, ANN and ensemble-ANN models

ANN is a data-driven modelling approach that addresses adsorption prediction and interpretation issues by employing dataset knowledge particular to an adsorbent–adsorbate combination. The standalone ANN frameworks extensively used Levenberg–Marquardt (LM) backpropagation training algorithm and hyperbolic tangent-linear activation functions to optimize the metal adsorption process on biomaterials systems (ESI, S2†). The LM algorithm incorporates the fast convergence ability of the Gauss–Newton algorithm and inherits the steepest descent method's stability to minimize the modelling error.[134] The role of activation function is critical in tuning the ANN model. The researchers have applied mainly hyperbolic tangent (tansig) activation function at the hidden layer as it centres each layer's output more or less around 0, which frequently aids in accelerating convergence.[135] The current developments in the field of machine learning demonstrate the potential of scaled exponential linear unit (SELU), rectified linear unit (ReLU) and exponential linear unit (ELU) to overcome the problems of overfitting and huge training dataset.[136] Since the experimental adsorption data set are not very big (<500 data points), scholars have usually selected classical activation functions for nonlinear mapping of data points. Future research can investigate the impact of varying dataset sizes, training algorithms, and activation functions on the quality of interactions and model performance.

The performance of standalone and ensembled ANN systems for simulating adsorptive eviction of metal ions using biomaterial adsorbents has also been studied along with traditional mathematical models (*e.g.* RSM, MLR, MNLR) as tabulated in Table 5. It was also reported that the ANN successfully optimized the metal adsorption process for datasets beyond the studied ranges.[48,57,62,98,99,137,138] These results validate their true generalization capability. In the case of a smaller dataset (<50 data points), the results predicted by ANN models very well matched the actual data points, demonstrating the ANN's suitability to decrease reagent use, which would impact the economic aspect of wastewater treatment.[138,139] The integration of evolutionary algorithms and fuzzy models with ANN has improved the predictive ability of ANN systems. This behaviour can be attributed to the knowledge of search algorithms to create multiple solutions to a given problem.[140] Each solution holds various parameters that can aid in enhancing the ANN efficiency. Fig. 5 sums up the predictive power of ensemble ANNs over standalone frameworks and traditional statistical models.

The authors acknowledged the capacity of the developed ANN models with metaheuristic optimizers to simulate the adsorption of metal ions on biomaterials. Yet, there is a need to explore these optimizers with a varied dataset on different metal pollutants with a clear explanation of the methodological phase for developing the research knowledge and comparing their capacity to deal with the stochastic, nonlinear complex data.

5. ANN frameworks for hybridizing classical adsorption models

5.1 Hybridized-ANN models

The process model development is an integral part of water treatment *via* adsorption. The classical means of modeling

Table 5 Comparison of different reports on standalone and ensembled ANN-based modelling methods for adsorptive eviction of distinct metal ions using biomaterial adsorbents[a]

Models	Model input	Model output	Performance metrics	Comments	Ref
ANN	Ion concentration, adsorbent weight, temperature, contact time and pH	Adsorption efficiency	MSE, R	Based on the batch experimental data, ANN reliably predicted the adsorption efficiency of Pb(II) on Antep pistachio shells	141
ANN	Temperature, particle size, ion concentration and pH	Adsorption efficiency	MSE, RE	ANN predicted the adsorptive eviction of Cu(II) using sawdust with a mean error within ±1%	142
ANN	Metal concentration, biomass dose, time and temperature	Adsorption efficiency	ARPE, R^2	ANN model displayed ~98% accuracy with the experimental As(III) adsorption on bacillus cereus biomass	143
ANN	Volume, ion concentration, adsorbent dose, contact time and pH	Sorption efficiency	MSE, R^2, MAE	pH of solution contributed the highest, and contact time contributed the least in describing the adsorption dynamics of lead ions on rice straw-based nanocellulose fibers	144
ANN	Contact time, initial arsenic concentration pH, and adsorbent dose	Sorption efficiency	MSE, R^2	The pH and volume of solution had the most and least degree of impact, respectively, on As(III) and As(V) removal using *Leucaena leucocephala* seed powder	145
ANN	Bias, pH, the dose of alginate nanoparticles, and contact time	Sorption efficiency	SSE, RE and R^2	ANN model showed good predictive performance of Ni(II) and Co(II) removal using alginate nanoparticles	55
ANN	Biomass dose, concentration, and time	Sorption efficiency	MSE	Initial concentration of adsorbate strongly affected the Cr(III) sorption efficiency, whereas treatment time influenced the Cr(VI) sorption on nanocrystalline cellulose	70
ANN	No. of adsorbents, adsorbent weights, pH, contact time, and ion concentration	Sorption efficiency	AARE, SD, MSE and R	ANN results showed better predictive performance for all the biomaterials, namely, coconut shell, neem leaves, hyacinth toots, rice husk, rice bran, rice straw, neem bark, and sawdust of teakwood	146
ANN	Residence time, ion concentration, adsorbent weight, pH and temperature	Adsorption efficiency and final pH	R	ANN response showed excellent agreement with the observed Ur (VI) adsorption results using polyacrylonitrile grafted potato starch	79
ANN	No. of adsorbents, time, flow rate, bed height, and initial concentration	Removal efficiency	AARE, SD, MSE and R	ANN with a single hidden layer predicts Pb(II) sorption efficiency with reasonable accuracy on multiple biomaterials, *i.e.* coconut shells, neem leaves, hyacinth roots, and rice wastes	147
ANN	pH, residence time, inoculum size and initial arsenic concentration	Removal efficiency	R^2, MSE	The distribution of model results closely fitted the As(III) and As(V) experimental data points using algal biomass, *i.e. Botryococcus braunii*	148
ANN	Adsorbent weight, pH, ion concentration, and residence time	Removal efficiency	R^2	ANN supplemented experimental results in a better explanation of Hg(II) adsorption on *Sargassum bevanom* biomass	149
ANN	Adsorbent weight, residence time, and ion concentration	Adsorption efficiency	R^2, MSE	The excellent values of R^2 (>0.99) showed the precision of ANN in predicting the adsorption of Pb(II), Cd(II) and Ni(II) on functionalized wood pulp	81
ANN, RSM	Residence time, adsorbent weight, and ion concentration	Adsorption efficiency	R^2, RMSE	ANN (3-9-2) accurately predicted the removal of Cu(II) and Pb(II) using nanocomposites derived from rice straw and Fe_3O_4 nanoparticles (R^2 = 0.95–0.99, RMSE = 0.95–1.87) with a negligible residual standard error of 0.02% as against RSM output	57
ANN	No. of adsorbents, adsorbent weight, ion concentration, pH adsorbent dose, time, initial concentration of ion and pH	Removal efficiency	R, AARE, SD and MSE	ANN was proved to be the best predictive model for Cr(VI) eradication from wastewater using multiple biosorbents, *i.e.* coconut shell powder, bamboo leaf, garlic peel, acid-treated rubber leaf, onion peel, mango, and jackfruit leaf	150

Table 5 (*Contd.*)

Models	Model input	Model output	Performance metrics	Comments	Ref
ANN	Bed depth, effluent concentration rate, flow rate, pH, time, and initial metal concentration	Removal efficiency	AARE, SD, MSE, R and χ^2	ANN response indicates its usefulness for predicting Cu(II) removal from wastewater using peanut and almond shells in a column adsorption system	151
ANN	Adsorbent weight, ion concentration, agitation speed and pH	Removal efficiency	R^2	ANN was found to predict the Cd(II) removal using Spirulina (Arthrospira) sp. with the best coefficient of determination	152
ANN	Residence time, adsorbent weight, ion concentration, particle size and pH	Adsorption efficiency	R^2	The ANN results predicted Cd(II) adsorption on gossypium barbadense waste with reasonable accuracy at epoch = 6	91
ANN	Particle size, ion concentration, temperature, and pH	Adsorption efficiency	R^2	ANN results predicted Cd(II) adsorption on moringa oleifera seed accurately	153
ANN	Walnut shell–rice husk ratio, calcination duration and temperature	Sorption efficiency	R^2	Adsorption of Cd on nano-magnetic walnut shell–rice husk	154
ANN, RSM	Residence time, ion concentration, particle size, pH, and adsorbent weight	Removal efficiency	R^2, MSE, SD	The study found an enormous potential of ANN over the quadratic mathematical model (deviation ~16.3%) to forecast Ni(II) adsorption on potamogeton pectinatus closer to the experimental response (R^2 = 0.9714, MSE = 1.4). Also, initial ion concentration has the highest and particle size has the most negligible influence on removal efficiency	155
ANN, RSM	Metal concentration, pH, adsorbent weight, and temperature	Removal efficiency	R^2	The study reported that the ANN model (4-4-1) performed well (R^2 = 0.9971) for the Cr(VI) adsorption on cyanobacterial biomass with diminished error values against RSM	48
ANN	Adsorption dose, ion concentration and pH	Removal efficiency	R^2	The chromium adsorption on *Borassus flabellifer* coir was modelled by ANN with a high coefficient of determination	156
ANN, RSM	Adsorption dose, ion concentration and pH	Removal efficiency	R^2, RMSE	The adsorptive removal of chromium using Flabellifer coir powder and Ragi husk powder was better simulated using the ANN scheme	157
ANN, MLR	Ion concentration, pH, residence time, and temperature	Adsorption capacity	R^2, RMSE	The dataset of chromium removal using maize bran was better modelled using the ANN framework	158
ANN	Adsorbent dosage, contact time, temperature, pH, metal ion concentration	Removal efficiency	R^2, MSE	An excellent fit between ANN output and experimental results was achieved in 188 iterations for As(III) adsorption on *Bacillus thuringiensis* strain WS3	159
ANN	Temperature, ion concentration, reaction time and adsorbent weight	Removal efficiency	R	The cadmium removal efficiency using activated oak waste showed a high correlation (>0.999) for the observed data with a negligible deviation	64
ANN	Initial metal ion concentration, time, adsorbent dose, and pH	Removal efficiency	MRE (%), MSE and R^2	ANN proved to be a valuable approach for modelling Cr(VI) biosorption using date palm fiber with a high coefficient of determination	160
ANN, MLR	pH, residence time, ion concentration and adsorbent weight	Removal efficiency	R^2	ANN showed better prediction potential (R^2 = 0.99) for Pb(II) removal using a carboxylate-functionalized walnut shell over conventional models	75
ANN	Temperature, pH, agitation rate, adsorbent dose, and contact time	Removal efficiency	R^2, MSE	The ANN architecture predicted chromium adsorption onto iron-doped rice husk more accurately than rice husk	71
ANN	pH, residence time, T-Fe_3O_4 nanocomposite dosage, and initial concentration	Removal efficiency	MAE, RMSE	ANN satisfactorily assisted in extracting the knowledge about the adsorption of lead ions on iron nanocomposites derived from Tangerine bio-waste with a small experimental data set	85

Table 5 (*Contd.*)

Models	Model input	Model output	Performance metrics	Comments	Ref
ANN	Adsorbent dose, bed depth, flow rate, pH, initial concentration, particle size, and treatment time	Adsorption capacity	R^2, RMSE	Adsorption time and bed depth were found to be the most and most minor influential parameters affecting Cu(II) adsorption on sunflower shells	161
ANN	Adsorbent dose, bed depth, flow rate, pH, initial concentration, particle size, and treatment time	Adsorption capacity	R^2, RMSE	Adsorption time and pH were found to be the most and least influential parameters affecting Co(II) uptake on sunflower shells	58
ANN, RSM	Temperature, adsorbent weight, contact time and pH	Adsorption capacity	R^2, RMSE	ANN proved to be a helpful tool for predicting Zn(II) adsorption from leachate ($R^2 = 0.99$, RMSE = 0.0029) on hazelnut shell	162
ANN, RSM	pH, temperature, ion concentration, biomass weight, bed depth and flow rate	Adsorption capacity	R^2	ANN response indicated its potential to simulate arsenic ions adsorption on rice polish in batch and column mode	138
ANN, RSM	pH, adsorbent dose, and temperature	Adsorption capacity	R^2, RMSE	ANN closely fitted with the arsenic adsorption results using black cumin over the RSM model	163
ANN	Ion concentration volume, residence time, pH and adsorbent weight	Adsorption efficiency	RMS, R^2	ANN best predicted the effect of interactions among multiple variables on the Pb(II) adsorption capacity using bacillus subtilis beads	164
ANN	Metal ion concentration, operating temperature, pH, agitation time, particle size and contact time	Adsorption capacity	R^2, MSE	The ANN displayed a compelling correlation between the predicted output and experimental response for cadmium adsorption on valonia tannin resin	165
ANN, RSM	Adsorbent weight, ion concentration and pH	Adsorption capacity	R^2, MSE	A high R^2 value confirmed the closeness between the predicted and observed values. The study reported the superiority of ANN over RSM in predicting Cu(II) adsorption capacity of flax meal	47
ANN, RSM	pH, temperature, residence time and ion concentration	Adsorption capacity and removal efficiency	R^2, SSE and ARE	ANN topology agreed excellently with the experimental data ($R^2 \sim 1$) at low average relative errors of 1.032 and 0.056, corresponding to nickel removal efficiency and uptake capacity using alginate composite beads	59
ANN	pH, temperature, ion concentration and residence time	Adsorption capacity	R^2	Neural architecture predicted the cobalt adsorption capacity of alginate-based nanocomposites nearer to the experimental observation	58
ANN	Adsorbent weight, ion concentration and pH	Adsorption capacity	R^2	ANN gave highly consistent results with the experimental zinc adsorption capacity of peanut shells	166
ANN	Ion concentration, residence time, pH and adsorbent weight	Adsorption capacity	R^2, MSE	ANN excellently estimated the potential of gundelia tournefortii to remove Pb(II) from synthetic wastewater	167
ANN, MLR	pH, nanoparticles mass, contact time, and initial concentration	Adsorption capacity	R^2, MSE	ANN accurately predicted simultaneous adsorption of the nickel and cobalt from wastewater using carboxymethyl-chitosan-bounded Fe_3O_4 nanoparticles. In addition, the study documented the superiority of ANN over MLR in predicting adsorption with the most negligible variation in error	99
ANN, MLR	Temperature, ion concentration, adsorbent weight, contact time and pH	Adsorption capacity	R^2, MSE	The ANN showed a firm fit with copper uptake capacity of raw guideline tournefortii results compared with conventional regression results	168
ANN	Equilibrium concentrations of the metal ions	Adsorption capacity	F_{obj}	ANN response of cadmium and zinc adsorption on sargassum filipendula fitted better than the classical adsorption models	169

Table 5 (*Contd.*)

Models	Model input	Model output	Performance metrics	Comments	Ref
ANN, RSM	Equilibrium concentrations of metal ions	Maximum adsorption capacity	R^2, MRE	ANN model response closely fitted with experimental isotherm points of Cr(VI), Zn(II) and Cu(II), adsorption on chitosan foamed structure, indicating good correctness	61
ANN	Adsorbent characteristics, metal ion properties, experimental isotherm and kinetics data	Kinetics and isotherm adsorption capacity	R	ANN that included both sorbent characteristics and metal ion properties as input variables produced the best results for Pb(II), Zn(II), Ni(II), and Cd(II) adsorption on cellulosic wastes (from jacaranda, nutshell, and plum kernels)	92
ANFIS	Ion concentration, adsorbent weight, hydroxyapatite concentration, pH, temperature, shaker velocity and time	Adsorption capacity	R^2, MSE	The ANFIS structure predicted the Pb(II) removal using hydroxy-apatite/chitosan composites with high accuracy	60
ANFIS, MLR	pH, initial concentration of copper, amount of date palm seeds	Adsorption capacity	R^2, MSE	The results indicated a greater potential of ANFIS to deal with copper adsorption data on date palm seeds in relation to the regression model	170
ANN, ANFIS	pH, temperature ion and concentration	Removal efficiency	R^2	The high R^2 (~0.99) indicated the applicability of both the models in the prediction of the mercury removal using vibrio parahaemolyticus PG02	171
ANFIS, RSM	Ion concentration, pH, and concentration of treatment solution	Adsorption capacity	R^2, SD	ANFIS predicted the maximum Pb(II) uptake with less than a 5% error deviation from the experimental values. In contrast, FFD showed a relatively weak prediction of biosorption capacity, chemically treated olive stone	84
ANFIS	Metal ion concentrations, wheat straw granulometry, temperature, contact time	Adsorption capacity	R^2, RMSE	The ANFIS architecture, after 15 iterations, showed high R^2 between the predicted and experimental results of Cr(VI) and Cu(II) adsorption on the wheat straw with diminished root means square error values	80
ANFIS	Contact time, nickel and cadmium ions concentration, adsorbent dose, pH, and particle size of adsorbent	Removal efficiency	R^2, RMSE	The results indicated a relatively more significant influence of pH and ion concentration on the Ni(II) and cadmium(II) removal efficiency using *Typha domingensis*	172
ANFIS	Adsorbent weight, residence time, pH, and ion concentration	Adsorption efficiency	R^2, RMSE	The biomass dose and pH were depicted as the most influential process parameters which affected the Cr(VI) sorption efficiency for date palm leaves and broad bean shoots, respectively	173
ANN, ANFIS,	2^3factorial design	Initial ion concentration, adsorbent dose, and pH			
	Adsorption efficiency	R^2, RMSE	The initial ion	concentration with the least training and checking error controlled the cadmium adsorption on rice straw, followed by the pH and adsorbent dose. The full factorial design also complemented the ANFIS results	129
ANN-GA, RSM	Temperature, ion concentration, pH, and residence time	Adsorption efficiency	R	The optimization results revealed the potential of ANN-GA (99.86%) to represent and explain actual Hg(II) adsorption data using yeast against the RSM (97.75%) model	45
ANN-GA	Contact time, pH, particle size and mixing speed	Removal efficiency	R^2, RE	A residual error of 1.3% was found between the observed Cu(II) adsorption on banana floret and model results, which validated the ANN-GA hybrid structure. In addition, the pH and time have the most significant influence on the removal efficiency	72

Table 5 (*Contd.*)

Models	Model input	Model output	Performance metrics	Comments	Ref
ANN-GA	Initial metal ion concentration and temperature	Removal efficiency and change in gibbs free energy	R, MSE	The optimization with GA resulted in a 92.9% of Pb(II) removal using thiosemicarbazide modified chitosan and -5 kJ mol^{-1} of gibbs energy change at 55 °C and 10 ppm of initial ion concentration	62
ANN-GA, MNLR	pH, bed depth, number of adsorbents, time, and flow rate	Removal efficiency	R, AARE, MSE and SD	The high correlation coefficient ($R = 0.9965$ to 0.9992) confirmed the model prediction accuracy of the chromium removal using mango, jackfruit, and rubber leaves prediction over MNLR.	174
ANN-GA	Adsorbent dose, pH, and contact time	Removal efficiency	R, MSE	The statistical indices hold minor variance (<5%) between the experimental and ANN output, indicating the great potential of the hybrid model to simulate thorium adsorption on chitosan-derived TiO_2 composites	175
ANN-GA, Taguchi design ANN-SA	Bed depth, flow rate, and ion concentration	Removal efficiency	R, RMSE	The results indicated better productivity of GA when compared with the Taguchi design, and SA optimizer outputs to model chromium removal using alginate immobilized *Sargassum* sp.	176
ANN-GWO, ANN-BR-GWO	Temperature, pH, ion concentration, and adsorbent dose	Adsorption efficiency	R^2, RMSE	FFNN model (trained with Bayesian-regularization (BR) algorithm) and optimized with GWO efficiently modelled the adsorption of Pb(II) and Co(II) ions on Rafsanjan pistachio shell	101
ANN-COA	Elution solvent, flow rate, the concentration of PAN [1-(2-pyridylazo)-2-naphthol], adsorbent dose, pH, and volume of elution solvent	Adsorption efficiency	R^2, RMSE	The ANN-COA model predicted the output with a small residual error of 1.3% and R^2 value of 0.9954 for the uranium adsorption using zinc oxide nanoparticles–chitosan	177

[a] R^2: coefficient of determination, MSE: mean square error, R: correlation coefficient, RMSE: root mean square error, AARE: absolute average relative error, SD: standard deviation, MRE: mean relative error, SSE: sum of square error, MAE: mean average error, ARE: average relative error, χ^2: chi-square, F_{obj}: objective function, ARPE: average relative percentage error, RMS: root mean square.

adsorption include calculating parameters related to isotherm, kinetics and thermodynamics through experimental values obtained at optimum conditions. However, the One Variable At a Time (OVAT) approach is applied to independently optimize the individual effect of adsorption variables such as contact time, pH, temperature, adsorbent dose and initial metals concentration.[178–181] Considering the impact of individual variables, analytical error and uncertainty associated with the traditional experimental approach, different AI models are used to improve the mathematical representations of adsorption process models. In this regard, Rodríguez-Romero *et al.*, 2020 hybridized the ANN with classical isotherm and kinetic equations to improve the arsenic adsorption capacity of carbon-enriched biomaterial.[211] The authors obtained the ANN-Langmuir model from the classical Langmuir functionality using initial metal concentration, pH and temperature as input parameters with sigmoid activation functions. Likewise, the other hybridized models were also obtained. The hybridized ANNs outperformed the traditional kinetics and isotherm models as portrayed in Fig. 6 where it is clear that the hybrid ANNs are less susceptible to error.

Only a few studies report using such a modelling strategy to remove fluoride ions, indicating a novel area of research.[182–184] ANN tools are easily used because they can establish dependencies and correlations between multiple variables. ANN architectures with equilibrium concentrations of metal toxins and temperature as net entrance data and metals adsorbed as the exit variables are processed to capture the best fit for the single and multicomponent adsorption process.[53] It is important to remark that similar ANN frameworks can be used to design multicomponent adsorption processes for metal removal at different operating conditions. The utility of AI has expanded with the hybridization of ANN with isotherm or kinetic equations to acquire pertinent adsorption parameters that are not possible using a standard model.[185]

Apart from isotherm and kinetics, estimating thermodynamic parameters of the adsorption process using ANN is an emerging field of research. Recently, Zaferani *et al.*, 2019 implemented ANN to recognize the standard Gibbs free energy changes (ΔG) related to Pb(II) adsorption process based on the changing temperature and initial metal concentration. The authors investigated different structures of ANN for modelling

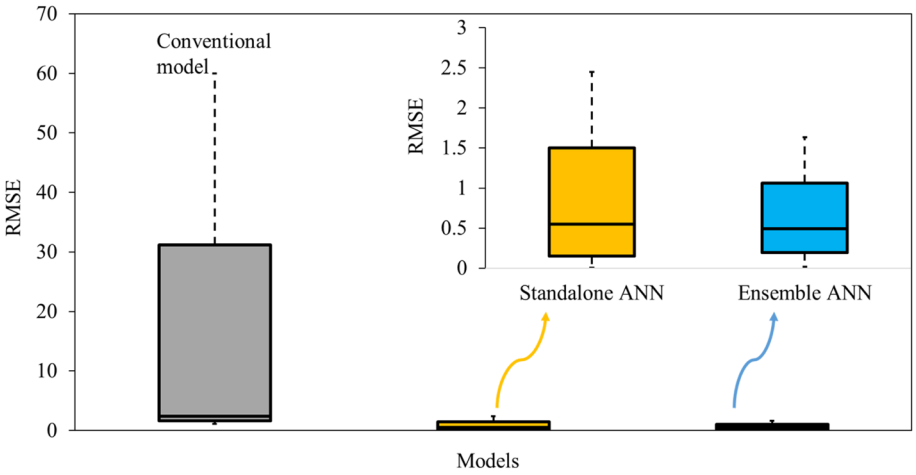

Fig. 5 Modelling error occurred in conventional, standalone and ensemble models for simulating adsorption on biomaterials (figure generated using the data from Section S5.6†).

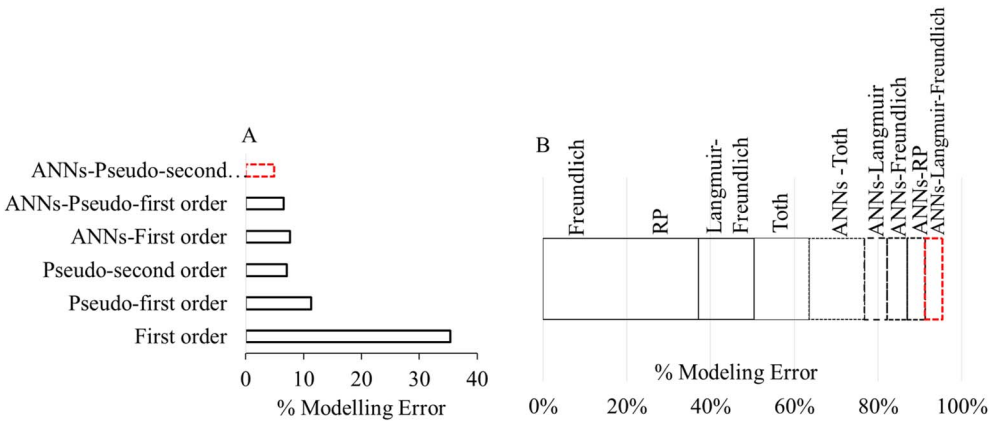

Fig. 6 Percent error in hybrid-ANN and traditional adsorption models using (A) kinetics, (b) isotherms (reproduced from ref. 102 with permission from [Elsevier], copyright [2020]).

ΔG and metal removal efficiency.[62] The results revealed that the minimum value of ΔG (-6 kJ K^{-1}) occurred at the highest temperature (55 °C) and the lowest initial Pb(II) concentration (10 ppm). The negative Gibbs free energy verified the spontaneity of the adsorption process. Limited studies explored the possibility of analyzing thermodynamics aspects of the adsorption process using ANN-framework. Much research is needed to create intelligent models that can predict the nature and viability of the adsorption process.

It should be emphasized that the parameters of conventional adsorption models are established by fitting specific experimental data. This indicates that the parameters of conventional adsorption models are constant for a given range of experimental conditions (Tables 1–3). On the other hand, ANN model parameters are derived through concurrent regression of all experimental observations.[186] Thus, hybrid adsorption model parameters are treated as nonlinear functions of the input variables used to train the artificial neural network, enhancing their adaptability and data correlation capabilities. These results demonstrated that using ANNs to estimate analytical adsorption equations parameters significantly improved modelling results.

5.2 Multicomponent adsorption

Wastewater is a matrix of multiple pollutants; therefore, developing a single technique for concurrent extraction of coexisting metallic impurities is critical. However, fabricating an adsorbent that considers the characteristics of all contaminants whose removal is required is challenging.[100,187] The process of multiple metal adsorption on biomaterials is usually studied in the column set-up in the laboratory and analyzed using breakthrough curves; but the existence of various metal pollutants in the feed makes modeling of breakthrough curves complex due to the pollutants' antagonistic, synergistic, and noninteractive tendencies.[188] Advanced models that illustrate multicomponent adsorption and the associated physics are part of the evolving research.[189] In this context, for the first time, Pauletto *et al.*, 2020 implemented ANN with a Bayesian regularization algorithm to investigate the antagonistic and

synergistic effects during the adsorption of dye (MB) and metals (Co(II)), Ni(II)) in single, binary and ternary mixtures on ultrasound modified chitin.[212] They optimized the input parameters (*i.e.* temperature and initial pollutants concentration) to simultaneously forecast the uptake capacity of individual adsorbates from a multicomponent system. The ANN-based simulations indicated that the optimized network of single component systems can be applied to model the equilibrium adsorption of cobalt (Co(II)), nickel (Ni(II), and methylene blue (MB) effectively ($R^2 = 0.99$) in multicomponent systems.

Simulating biomaterial systems for multi-metals adsorption is an emerging field of study that has the potential to computationally design cost-effective adsorbents with tailored properties to effectively treat industrial effluents without the need for multiple stages involved in adsorption system design. Other advantages of this technique include cost reduction and time savings to generate high-efficiency adsorption systems that simultaneously treat diverse water pollutants. The future studies can analyse the application of ANN integrated with nature and human-inspired metaheuristic optimization algorithms for the adsorptive eviction of multiple species from BMs.

6. Sensitivity analysis

The ANN frameworks' limitations is their inability to comprehend the physico-chemistry behind the adsorption behaviour; therefore, their uninformed application to a sorption system without paying attention to the physicochemical characteristics could result in dubious outcomes. To address this concern, researchers used a sensitivity analysis of ANN to determine the impact of experimental factors on the adsorption of metal ions. A sensitivity analysis of the developed ANN allows assessment of the input attributes as per their impact on the output response. In the literature, the Weights method has usually been employed to examine the sensitivity of the adsorption process and identify the most significant parameters that influence the adsorption performance (ANN output).[190] The mathematical presentation of network weights for determining the relative weights of input parameters is given in ESI, Section S6.†

In the biomaterial adsorption system, pH, initial concentration of adsorbate, and contact time were the most critical process variables that impacted the metal adsorption on biomaterials. Since the pH alters the ionic strength and affects the ionization of metals onto biomaterials, the contact time between adsorbate and adsorbent affects the available active sites,[213,214] whereas the concentration of metal affects the interaction of metal ions with the available binding sites. Furthermore, it was found that the quantity and quality of the biomaterial adsorbed significantly impacted the effectiveness of the adsorption process.[73] The medium of aqueous solutions also affected the adsorptive removal of metal ions. For example, the presence of organic matter and its derivatives or salinity might change the biomaterials' surface characteristics and block the metals' adsorption on biomaterials. Considering the wastewater treatment plants, the quantity of biomaterial required for successful adsorption of metal adsorbates at a fixed initial concentration serves importance from an economic perspective. The process cost will be lowered when sufficient adsorption is attained with a small biomaterial dose. Since the selling cost of natural biomaterials is very low, but their excessive usage can increase their waste disposal costs, while inefficient use can increase the process cost. Thus, understanding how operating variables affect the adsorption using ANN approach will aid in the appropriate process design, scale-up and optimization of an industrial adsorption process. In

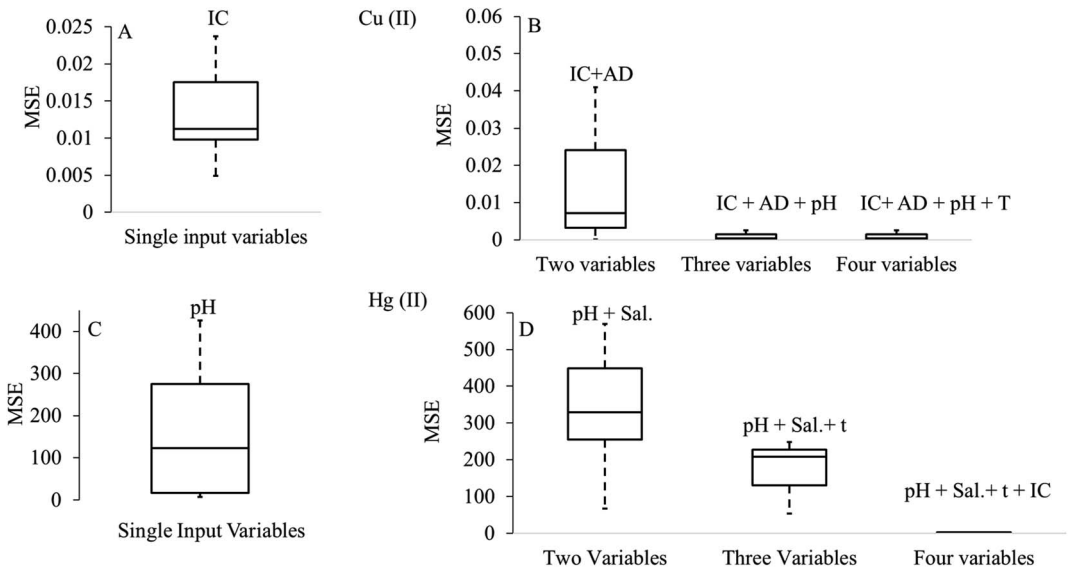

Fig. 7 Influence of single and combinations of input variables on the ANN response. *AD = adsorbent dose, IC = initial metal ion concentration, T = temperature, CT = contact time and Sal. = salinity of aqueous medium. (A and B) were generated using the data obtained from ref. 168 with permission from [Elsevier], copyright [2019], while (C and D) were generated using the data obtained from ref. 77 with permission from [Springer Nature], copyright [2018].

addition, implementing neural networks will process monitoring and control, save time, and lower costs.

Besides determining the contribution of single input parameters, researchers studied the conjugate effects of multiple input parameters on ANN prediction. Fig. 7 shows the significant decrement in the prediction error (MSE) for copper and mercury removal with the increasing combinations of input parameters. Fig. 7 shows that as the number of input variables in the group rose, the values of MSE decreased because of the strong effect of all parameters on adsorption capacity. Although the influence of process variables has been explored widely, the contribution of biomaterial characteristics in terms of their lignin–cellulose–hemicellulose content, pore size distribution, particle size and surface area on the predictive ANN response has not been fully explored. The information about the influence of the above-mentioned attributes can benefit technologists and engineers in selecting and designing adsorption systems.

The sensitivity analysis was primarily reported in studies focusing on standalone ANN frameworks, which followed a gradient-based optimization scheme (details of studies in Table 5). Thus a comparative analysis of metaheuristic-based ensemble models and ANN can be carried out in future to predict the relative contribution of adsorption variables on the metal adsorption efficacy of BMs. Apart from Weights methods, there are other methods of calculating sensitivity and feature importance, *e.g.*, partial derivate algorithm,[191] input perturbation algorithm,[192] profile[193] and stepwise method.[194] There is a need to test the sensitivity of ANN response using different approaches to determine the optimal sensitivity criteria, which could be the focus of future studies.

7. Challenges and advancements in ANN technology for the removal of metals

The main disadvantage of ANN is its black box and empirical character. The connection link between neurons is denoted by weights, which are difficult to represent mathematically. The contribution of a specific input variable to the outcome of ANN is identified based on its numeric value and sign of the associated weight. The higher the weight value, the greater the independent variable's contribution to the expected response. The effects of negative weights on neurons are conflicting. Thus, positive outcomes have a synergistic impact on the neurons, boosting the value of the response, whereas negative outcomes have the opposite effect and decrease the expected value of the output (Section 6).

Although the above-discussed sections demonstrate ANN as a superior approach to the traditional models due to less formal statistical training requirements, detection of complex nonlinear relationships and all possible interactions between the variables, there is a need to develop novel strategies that can provide in-depth analysis of adsorption phenomena in terms of surface interactions and associated adsorption energy. Recent research by Fagundez *et al.*, 2021 offered novel hybrid ANN-isotherms for simultaneous estimation of isotherm and thermodynamics parameters to predict metal uptake capacity and associated thermodynamic parameters of various zeolites under different temperature conditions.[215] The utility of molecular simulations combined with ANN has recently been reported as a valuable modelling strategy to gain insights into the mechanism of heavy metal adsorption on graphene nanocomposites with high accuracy.[195] The computation models based on density functional theory (DFT) have been employed to determine the adsorption energies on solid surfaces. However, developing a neural network-based scheme that can predict surface energies on sorbents can assist in optimizing the relative stability of adsorbent surfaces for spontaneous adsorption of targeted metal pollutants on available active sites.[196–199] In addition to developing new computational strategies, the researchers emphasize on meaningful experimental results to understand the equilibrium, saturation and regenerative potential of adsorption systems from a chemical science point of view.[56,200]

The possibility of overfitting is the second major issue that needs to be addressed by researchers while applying ANN algorithms to predict biomaterial systems' efficacy for wastewater treatments.[91,92] To prevent the over-parameterization and over-training of the ANN system, researchers have advocated the implementation of emerging activation functions (*e.g.*, SeLU, ReLU).[201,202] Using simple models (*e.g.*, AdaBoost) ensures the generalizability of output in the small dataset.[203]

It is commonly recognized that a smaller error value is better for optimum network learning; however, it may be possible that the network training stops due to getting stuck in local minima. Such situations call for hybridizing the ANN framework with novel evolutionary algorithms. Recently, Ke *et al.*, 2021 proposed novel ANN-based-surrogate models (*i.e.*, BA-ANN, SVM-ANN, RF-ANN, M5Tree-GP, M5Tree-ANN and GP-ANN) for predicting metal removal efficiency based on characteristics of carbonaceous materials, source of metal and environmental conditions.[107] The particle swarm optimizer (PSO) has been coupled with ANN to predict the dye and copper removal efficiency using graphene oxide-based nanocomposites and pomelo-peel-based carbonaceous material.[204,205]

8. Prospective scope

❖ Based on the reviewed literature on metal ion modelling using ANN, estimating the absorption capability of biomaterials other than polysaccharide-derived materials requires additional research.

❖ Models discussed were prepared and assessed based on metals present in synthetic solutions. The natural wastewater or water system is a complex matrix where various pollutants co-exist. The influence of co-existing metal pollutants in natural systems on the adsorption behaviour *via* ANN has not been fully explored. Thus, there is a greater scope of research in this domain.

❖ Although ANN-based models provided a better fit than static adsorption models, the literature lacked sufficient research on the development of ANN systems that can best

describe the breakthrough curves against dynamic adsorption models such as Thomas, Bohart–Adams and Yoon–Nelson models. Future research should demonstrate the performance of neural networks against dynamic adsorption models to forecast breakthroughs.

❖ As per the principles of circular economy, the reuse and recyclability of biomaterial systems are essential. A vast development of ANN models has predicted pollutant removal efficiency; however, little attention has yet been given to developing intelligent systems that can optimize the dose of eluting agents for maximum regeneration of adsorbent materials. Modelling desorption processes can allow further utilization and effective management of spent adsorbent materials.

❖ ANNs have been chiefly applied to model the removal of heavy metals and dyes. But the potential of bioadsorbents to treat emerging contaminants such as per- and polyfluoroalkyl substances (PFAS) and rare earth metals (*e.g.*, neodymium, cerium, and lanthanum) *via* adsorption needs attention for advancements in adsorption systems design.

❖ Environmental remediation occurs in different climate conditions. Also, the wastewater being processed for reuse can be at varying temperatures. In such situations, modelling thermodynamic aspects of the adsorption process can give crucial information related to the efficacy of biomaterials and the feasibility of adsorption phenomena for a broad spectrum of temperatures.

❖ ANN results need to be compared with the latest machine learning models, which are not yet explored for simulating adsorption processes such as super learning, decision tree, deep learning, and data mining. These models have provided promising solutions for various problems related to environmental engineering; however, they are yet to be assessed for wastewater treatment applications.

9. Conclusion

Metal pollution treatment is essential to prevent waste metals' bioaccumulation, environmental pollution, and soil degradation. Biomaterials act as a versatile and cost-effective system for removing metals from wastewater. Different chemical and physical modification methods of natural biomaterials can improve their metal adsorption efficiency, but conventional laboratory-based research has yet to describe multicomponent adsorption systems comprehensively. An artificial neural network can automate the adsorption process to optimize process variables and adsorbent fabrication pathways for increasing metal removal efficiency. Furthermore, ANN frameworks can generate hybrid isotherm and kinetic models that minimize error and accurately model an efficient, rapid, and cost-effective multicomponent system for metal removal. The application of ANN-based models leads to a better understanding of biomaterials' efficiency, energy, time and economic benefits. The thermodynamic aspects of metal adsorption to improve environmental water quality and applications in water reuse is a burgeoning field of research. The challenges of ANN can be briefly summarized as a) collecting experimentally characterized data to filter and identify specific metal contaminants in the complex matrix of water; and b) establishing ensemble models to assist in solving local minima problems, thereby improving the prediction efficiency of ANN. The intervention of ANN demonstrated robustness and rigour in simulating adsorptive eviction of metal ions using BMs, which could be expanded for other organic and emergent pollutants.

Disclaimer

The research presented was not performed or funded by EPA and was not subject to EPA's quality system requirements. The views expressed in this article are those of the author(s) and do not necessarily represent the views or the policies of the US Environmental Protection Agency.

Author contributions

Amrita Nighojkar: conceptualization, investigation, data analysis, visualization, writing – original draft; Karl Zimmermann: data analysis, writing – review & editing; Mohamed Ateia: visualization, writing – review & editing; Benoit Barbeau: writing – review & editing; Madjid Mohseni: writing – review & editing; Satheesh Krishnamurthy: writing – review & editing; Fuhar Dixit: investigation, data analysis, visualization, writing – original draft; Balasubramanian Kandasubramanian: conceptualization, supervision, project administration.

Conflicts of interest

The authors declare that they have no known competing financial interests or personal relationships that could have appeared to influence the work reported in this paper.

Abbreviations

AARE	Absolute average relative error
AD	Adsorbent dose
AI	Artificial intelligence
ANFIS	Adaptive neuro-fuzzy inference system
ANN	Artificial neural networks
ANN-COA	Cuckoo optimized hybridized neural network
ANN-GA	Genetic algorithm hybridized neural network
ANN-GWOA	Wolf optimized hybridized neural network
ANN-SA	Simulated annealing hybridized neural network
ARPE	Average relative percentage error
BD	Bed depth
BR	Bayesian regularization
C_e	Equilibrium concentration
COA	Cuckoo optimization algorithm
CT	Contact time
DA	DIRECT algorithm
FFNN	Feed forward neural network
FIS	Fuzzy inference system
FR	Flow rate
GA	Genetic algorithm
GD	Gradient descent

GWO	Grey Wolf optimizer
GWOA	Grey Wolf optimization algorithm
IC	Initial metal ion concentration
LM	Levenberg-Marquardt
MAE	Mean average error
MAPE	Mean absolute percentage error
MNLR	Nonlinear multiple linear regression
MRE	Mean relative error
MSE	Mean square error
NLR	Nonlinear regression
PS	Particle size
R	Correlation coefficient
R^2	Coefficient of determination
r% Ads	Correlation coefficient for % adsorption
R^2	Coefficient of determination
RMSE	Root mean square error
Rprop	Resilient backpropagation
RSM	Response surface methodology
SA	SIMPLEX algorithm
SCG	Scaled conjugate gradient
SD	Standard deviation
SDR	Standard deviation ratio
SSE	Sum of square error
T	Temperature
TAAE%	Total mean of absolute error%
VS	Volume of solution
y_m	Predicted value
y_e	Experimental value

Acknowledgements

Fuhar Dixit and Karl Zimmermann are Natural Sciences and Engineering Council of Canada's Vanier Scholars. The authors would further like to acknowledge Sharan Vasvani (Faculty of Computing Science, Simon Fraser University, Canada) for reviewing the manuscript and providing valuable feedback.

References

1 *UN-Water, Scarcity, UN-Water*, **https://www.unwater.org/water-facts/scarcity/**, accessed July 22, 2022.
2 S. Bolisetty, M. Peydayesh and R. Mezzenga, Sustainable technologies for water purification from heavy metals: review and analysis, *Chem. Soc. Rev.*, 2019, **48**, 463–487.
3 R. Chakraborty, A. Asthana, A. K. Singh, B. Jain and A. B. H. Susan, Adsorption of heavy metal ions by various low-cost adsorbents: a review, *Int. J. Environ. Anal. Chem.*, 2022, **102**, 342–379.
4 R. Rashid, I. Shafiq, P. Akhter, M. J. Iqbal and M. Hussain, A state-of-the-art review on wastewater treatment techniques: the effectiveness of adsorption method, *Environ. Sci. Pollut. Res.*, 2021, **28**, 9050–9066, DOI: **10.1007/s11356-021-12395-x**.
5 A. Zehra, M. Meena, P. Swapnil, N. A. Raytekar and R. S. Upadhyay, Sustainable approaches to remove heavy metals from water, *Microb. Biotechnol. Basic Res. Appl.*, 2020, 127–146.
6 N. L. Torad, A. Takahashi, M. Kawakami, T. Kawamoto and H. Tanaka, Decontamination of very dilute Cs in seawater by a coagulation–precipitation method using a nanoparticle slurry of copper hexacyanoferrate, *Environ. Sci. Water Res. Technol.*, 2019, **5**, 1328–1338, DOI: **10.1039/C9EW00259F**.
7 A. Nighojkar, V. K. Sangal, F. Dixit and K. Balasubramanian, Sustainable conversion of saturated adsorbents (SAs) from wastewater into value-added products: future prospects and challenges with toxic per- and polyfluoroalkyl substances (PFAS), *Environ. Sci. Pollut. Res.*, 2022, **29**, 78207–78227, DOI: **10.1007/s11356-022-23166-7**.
8 V. U. Kavitha and B. Kandasubramanian, Tannins for wastewater treatment, *SN Appl. Sci.*, 2020, **2**, 1–21, DOI: **10.1007/s42452-020-2879-9**.
9 F. Dixit, K. Zimmermann, R. Dutta, N. J. Prakash, B. Barbeau, M. Mohseni and B. Kandasubramanian, Application of MXenes for water treatment and energy-efficient desalination: a review, *J. Hazard. Mater.*, 2022, **423**, 127050.
10 A. Purabgola, N. Mayilswamy and B. Kandasubramanian, Graphene-based TiO2 composites for photocatalysis & environmental remediation: synthesis and progress, *Environ. Sci. Pollut. Res.*, 2022, 1–21.
11 K. V. Udayakumar, P. M. Gore and B. Kandasubramanian, Foamed materials for oil-water separation, *Chem. Eng. J. Adv.*, 2021, **5**, 100076.
12 M. N. Issac and B. Kandasubramanian, Review of manufacturing three-dimensional-printed membranes for water treatment, *Environ. Sci. Pollut. Res.*, 2020, **27**, 36091–36108.
13 P. M. Gore, P. Gawali, M. Naebe, X. Wang and B. Kandasubramanian, Polycarbonate and activated charcoal-engineered electrospun nanofibers for selective recovery of oil/solvent from oily wastewater, *SN Appl. Sci.*, 2020, **2**, 1–13.
14 A. K. Nighojkar, A. Vijay, A. Kumavat, S. Gupta, R. K. Satankar and A. Plappally, Use of marble and iron waste additives for enhancing arsenic and E. coli contaminant removal capacity and strength of porous clay ceramic materials for point of use drinking water treatment, *Desalination Water Treat.*, 2019, **157**, 290–302.
15 C. Shen, Y. Zhao, W. Li, Y. Yang, R. Liu and D. Morgen, Global profile of heavy metals and semimetals adsorption using drinking water treatment residual, *Chem. Eng. J.*, 2019, **372**, 1019–1027.
16 J. Febrianto, A. N. Kosasih, J. Sunarso, Y.-H. Ju, N. Indraswati and S. Ismadji, Equilibrium and kinetic studies in adsorption of heavy metals using biosorbent: a summary of recent studies, *J. Hazard. Mater.*, 2009, **162**, 616–645.
17 S. Rastogi and B. Kandasubramanian, Progressive trends in heavy metal ions and dyes adsorption using silk fibroin composites, *Environ. Sci. Pollut. Res.*, 2020, **27**, 210–237.
18 M. I. U. Hoque, Y. Yamauchi, R. Naidu, R. Holze, R. Saidur, Q. Qu, M. M. Rahman, N. L. Torad, M. S. A. Hossain and M. Kim, A facile synthesis of hematite nanorods from rice

starch and their application to Pb (II) ions removal, *ChemistrySelect*, 2019, **4**, 3730–3736.
19 N. L. Torad, R. Kanai, K. Ishikawa, R. Kamimura, T. Kawamoto and H. Tanaka, The development of a rapid monitoring method for radiocesium in seawater in the Fukushima region, *Environ. Sci. Water Res. Technol.*, 2022, **8**, 1547–1560, DOI: **10.1039/D2EW00211F**.
20 N. L. Torad, M. Hu, S. Ishihara, H. Sukegawa, A. A. Belik, M. Imura, K. Ariga, Y. Sakka and Y. Yamauchi, Direct Synthesis of MOF-Derived Nanoporous Carbon with Magnetic Co Nanoparticles toward Efficient Water Treatment, *Small*, 2014, **10**, 2096–2107, DOI: **10.1002/smll.201302910**.
21 P. Cheng, M. Kim, H. Lim, J. Lin, N. L. Torad, X. Zhang, Md. S. A. Hossain, C.-W. Wu, C. Wang, J. Na and Y. Yamauchi, A General Approach to Shaped MOF-Containing Aerogels toward Practical Water Treatment Application, *Adv. Sustain. Syst.*, 2020, **4**, 2000060, DOI: **10.1002/adsu.202000060**.
22 A. Pillai and B. Kandasubramanian, Carbon xerogels for effluent treatment, *J. Chem. Eng. Data*, 2020, **65**, 2255–2270.
23 A. K. Nighojkara, A. K. Agrawalb, B. Singhc, S. Guptaa, R. K. Satankara, J. M. Oommena, L. Davea, M. Sharifd, A. B. O. Soboyejoe and A. Plappallya, Establishing correlations among pore structure, surface roughness, compressive strength, and fracture toughness of ceramic water filters local to Rajasthan, India, *Water Treat.*, 2019, **157**, 332–341.
24 M. Abali, A. Ait Ichou, A. Zaghloul, M. Chiban, F. Sinan and M. Zerbet, Evaluation and improvement of the WWTP performance of an agricultural cooperative by adsorption on inert biomaterial: case of orthophosphate, nitrate and sulfate ions, *Appl. Water Sci.*, 2022, **12**, 1–9.
25 A. Subash, M. Naebe, X. Wang and B. Kandasubramanian, Biopolymer – a sustainable and efficacious material system for effluent removal, *J. Hazard. Mater.*, 2023, **443**, 130168, DOI: **10.1016/j.jhazmat.2022.130168**.
26 P. M. Gore, M. Naebe, X. Wang and B. Kandasubramanian, Nano-fluoro dispersion functionalized superhydrophobic degummed & waste silk fabric for sustained recovery of petroleum oils & organic solvents from wastewater, *J. Hazard. Mater.*, 2022, **426**, 127822.
27 N. Mayilswamy and B. Kandasubramanian, Green composites prepared from soy protein, polylactic acid (PLA), starch, cellulose, chitin: a review, *Emerg. Mater.*, 2022, **5**, 727–753, DOI: **10.1007/s42247-022-00354-2**.
28 P. M. Gore, M. Naebe, X. Wang and B. Kandasubramanian, Bioinspired and Natural Materials for Oil/Water Separation, in *Oil– Water Mix. Emuls. Vol. 2 Adv. Mater. Sep. Treat.*, ACS Publications, 2022, pp. 107–123.
29 C. Zinge and B. Kandasubramanian, Nanocellulose based biodegradable polymers, *Eur. Polym. J.*, 2020, **133**, 109758.
30 P. M. Gore, M. Naebe, X. Wang and B. Kandasubramanian, Silk fibres exhibiting biodegradability & superhydrophobicity for recovery of petroleum oils from oily wastewater, *J. Hazard. Mater.*, 2020, **389**, 121823, DOI: **10.1016/j.jhazmat.2019.121823**.
31 A. Rajeswari, E. J. S. Christy and A. Pius, Biopolymer blends and composites: processing technologies and their properties for industrial applications, in *Biopolym. Their Ind. Appl.*, Elsevier, 2021, pp. 105–147.
32 A. E. Ali, Z. Z. Chowdhury, R. F. Rafique, R. Ikram, A. N. M. Faisal, S. Shibly, A. Barua, Y. A. Wahab and B. M. Jan, Science and Technology Roadmap for Adsorption of Metallic Contaminants from Aqueous Effluents Using Biopolymers and Its' Derivatives, in *Adv. Ind. Wastewater Treat. Reclam. Water*, Springer, 2022, pp. 165–196.
33 Z. Xiang, N. Tang, X. Jin and W. Gao, Fabrications and applications of hemicellulose-based bio-adsorbents, *Carbohydr. Polym.*, 2021, 118945.
34 P. D. Bhalara, D. Punetha and K. Balasubramanian, Kinetic and isotherm analysis for selective thorium (IV) retrieval from aqueous environment using eco-friendly cellulose composite, *Int. J. Environ. Sci. Technol.*, 2015, **12**, 3095–3106.
35 S. Sharma, K. Balasubramanian and R. Arora, Adsorption of arsenic (V) ions onto cellulosic-ferric oxide system: kinetics and isotherm studies, *Desalination Water Treat.*, 2016, **57**, 9420–9436.
36 N. Singh and K. Balasubramanian, An effective technique for removal and recovery of uranium (VI) from aqueous solution using cellulose–camphor soot nanofibers, *RSC Adv.*, 2014, **4**, 27691–27701.
37 K. Thakur, A. Rajhans and B. Kandasubramanian, Starch/PVA hydrogels for oil/water separation, *Environ. Sci. Pollut. Res.*, 2019, **26**, 32013–32028.
38 P. D. Bhalara, K. Balasubramanian and B. S. Banerjee, Spider–web textured electrospun composite of graphene for sorption of Hg (II) ions, *Mater. Focus*, 2015, **4**, 154–163.
39 S. Rastogi and B. Kandasubramanian, Application of electrospun materials in water treatment, *Electrospun Mater. Allied Appl.*, 2020, 151–183.
40 P. M. Gore, M. Naebe, X. Wang and B. Kandasubramanian, Progress in silk materials for integrated water treatments: Fabrication, modification and applications, *Chem. Eng. J.*, 2019, **374**, 437–470.
41 A. Rajhans, P. M. Gore, S. K. Siddique and B. Kandasubramanian, Ion-imprinted nanofibers of PVDF/1-butyl-3-methylimidazolium tetrafluoroborate for dynamic recovery of europium (III) ions from mimicked effluent, *J. Environ. Chem. Eng.*, 2019, **7**, 103068.
42 R. R. Gonte, G. Shelar and K. Balasubramanian, Polymer–agro-waste composites for removal of Congo red dye from wastewater: adsorption isotherms and kinetics, *Desalination Water Treat.*, 2014, **52**, 7797–7811.
43 N. Ali, A. Khan, S. Nawaz, M. Bilal, S. Malik, S. Badshah and H. M. Iqbal, Characterization and deployment of surface-engineered chitosan-triethylenetetramine nanocomposite hybrid nano-adsorbent for divalent cations decontamination, *Int. J. Biol. Macromol.*, 2020, **152**, 663–671.
44 M. H. Dehghani, R. R. Karri, E. C. Lima, A. H. Mahvi, S. Nazmara, A. M. Ghaedi, M. Fazlzadeh and S. Gholami, Regression and mathematical modeling of fluoride ion

adsorption from contaminated water using a magnetic versatile biomaterial & chelating agent: insight on production & experimental approaches, mechanism and effects of potential interferers, *J. Mol. Liq.*, 2020, **315**, 113653.

45 E. A. Dil, M. Ghaedi, G. R. Ghezelbash, A. Asfaram, A. M. Ghaedi and F. Mehrabi, Modeling and optimization of Hg2+ ion biosorption by live yeast Yarrowia lipolytica 70562 from aqueous solutions under artificial neural network-genetic algorithm and response surface methodology: kinetic and equilibrium study, *RSC Adv.*, 2016, **6**, 54149–54161.

46 S. Mohan, Y. Singh, D. K. Verma and S. H. Hasan, Synthesis of CuO nanoparticles through green route using citrus limon juice and its application as nanosorbent for Cr(VI) remediation: process optimization with RSM and ANN-GA based model, *Process Saf. Environ. Prot.*, 2015, **96**, 156–166, DOI: 10.1016/j.psep.2015.05.005.

47 D. Podstawczyk, A. Witek-Krowiak, A. Dawiec and A. Bhatnagar, Biosorption of copper (II) ions by flax meal: empirical modeling and process optimization by response surface methodology (RSM) and artificial neural network (ANN) simulation, *Ecol. Eng.*, 2015, **83**, 364–379.

48 S. Sen, S. Nandi and S. Dutta, Application of RSM and ANN for optimization and modeling of biosorption of chromium (VI) using cyanobacterial biomass, *Appl. Water Sci.*, 2018, **8**, 1–12.

49 A. Asfaram, M. Ghaedi and G. R. Ghezelbash, Biosorption of Zn2+, Ni2+ and Co2+ from water samples onto Yarrowia lipolytica ISF7 using a response surface methodology, and analyzed by inductively coupled plasma optical emission spectrometry (ICP-OES), *RSC Adv.*, 2016, **6**, 23599–23610.

50 D. S. P. Franco, F. A. Duarte, N. P. G. Salau and G. L. Dotto, Analysis of indium (III) adsorption from leachates of LCD screens using artificial neural networks (ANN) and adaptive neuro-fuzzy inference systems (ANIFS), *J. Hazard. Mater.*, 2020, **384**, 121137, DOI: 10.1016/j.jhazmat.2019.121137.

51 R. Gomez-Gonzalez, F. J. Cerino-Córdova, A. M. Garcia-León, E. Soto-Regalado, N. E. Davila-Guzman and J. J. Salazar-Rabago, Lead biosorption onto coffee grounds: Comparative analysis of several optimization techniques using equilibrium adsorption models and ANN, *J. Taiwan Inst. Chem. Eng.*, 2016, **68**, 201–210, DOI: 10.1016/j.jtice.2016.08.038.

52 P. R. Souza, G. L. Dotto and N. P. G. Salau, Artificial neural network (ANN) and adaptive neuro-fuzzy interference system (ANFIS) modelling for nickel adsorption onto agro-wastes and commercial activated carbon, *J. Environ. Chem. Eng.*, 2018, **6**, 7152–7160.

53 P. S. Pauletto, G. L. Dotto and N. P. G. Salau, Optimal artificial neural network design for simultaneous modeling of multicomponent adsorption, *J. Mol. Liq.*, 2020, **320**, 114418, DOI: 10.1016/j.molliq.2020.114418.

54 S. Hokkanen, A. Bhatnagar and M. Sillanpää, A review on modification methods to cellulose-based adsorbents to improve adsorption capacity, *Water Res.*, 2016, **91**, 156–173.

55 A. Esmaeili and A. A. Beni, Novel membrane reactor design for heavy-metal removal by alginate nanoparticles, *J. Ind. Eng. Chem.*, 2015, **26**, 122–128.

56 M. Khajeh and E. Jahanbin, Application of cuckoo optimization algorithm–artificial neural network method of zinc oxide nanoparticles–chitosan for extraction of uranium from water samples, *Chemom. Intell. Lab. Syst.*, 2014, **135**, 70–75.

57 R. Khandanlou, H. R. F. Masoumi, M. B. Ahmad, K. Shameli, M. Basri and K. Kalantari, Enhancement of heavy metals sorption via nanocomposites of rice straw and Fe3O4 nanoparticles using artificial neural network (ANN), *Ecol. Eng.*, 2016, **91**, 249–256.

58 M. R. Kowsari, H. Sepehrian, M. Mahani and J. Fasihi, Cobalt (II) adsorption from aqueous solution using alginate-SBA-15 nanocomposite: kinetic, isotherm, thermodynamic studies and neural network modeling, *Mater. Focus*, 2016, **5**, 91–99.

59 A. A. Oladipo and M. Gazi, Nickel removal from aqueous solutions by alginate-based composite beads: central composite design and artificial neural network modeling, *J. Water Process Eng.*, 2015, **8**, e81–e91.

60 A. Sadeghizadeh, F. Ebrahimi, M. Heydari, M. Tahmasebikohyani, F. Ebrahimi and A. Sadeghizadeh, Adsorptive removal of Pb (II) by means of hydroxyapatite/chitosan nanocomposite hybrid nanoadsorbent: ANFIS modeling and experimental study, *J. Environ. Manage.*, 2019, **232**, 342–353.

61 E. Tomczak, Application of ANN and EA for description of metal ions sorption on chitosan foamed structure—equilibrium and dynamics of packed column, *Comput. Chem. Eng.*, 2011, **35**, 226–235.

62 S. P. G. Zaferani, M. R. S. Emami, M. K. Amiri and E. Binaeian, Optimization of the removal Pb (II) and its Gibbs free energy by thiosemicarbazide modified chitosan using RSM and ANN modeling, *Int. J. Biol. Macromol.*, 2019, **139**, 307–319.

63 B. K. Nath, C. Chaliha and E. Kalita, Iron oxide permeated mesoporous rice-husk nanobiochar (IPMN) mediated removal of dissolved arsenic (As): chemometric modelling and adsorption dynamics, *J. Environ. Manage.*, 2019, **246**, 397–409.

64 A. Takdastan, S. Samarbaf, Y. Tahmasebi, N. Alavi and A. A. Babaei, Alkali modified oak waste residues as a cost-effective adsorbent for enhanced removal of cadmium from water: isotherm, kinetic, thermodynamic and artificial neural network modeling, *J. Ind. Eng. Chem.*, 2019, **78**, 352–363.

65 S. Ullah, M. A. Assiri, M. A. Bustam, A. G. Al-Sehemi, F. A. Abdul Kareem and A. Irfan, Equilibrium, kinetics and artificial intelligence characteristic analysis for Zn (II) ion adsorption on rice husks digested with nitric acid, *Paddy Water Environ.*, 2020, **18**, 455–468.

66 M. Zhu, F. Li, W. Chen, X. Yin, Z. Yi and S. Zhang, Adsorption of U (VI) from aqueous solution by using KMnO4-modified hazelnut shell activated carbon:

characterisation and artificial neural network modelling, *Environ. Sci. Pollut. Res.*, 2021, **28**, 47354–47366.

67 S. Chakrabarty and H. P. Sarma, Heavy metal contamination of drinking water in Kamrup district, Assam, India, *Environ. Monit. Assess.*, 2011, **179**, 479–486, DOI: 10.1007/s10661-010-1750-7.

68 T. Khan, M. H. Isa, M. R. U. Mustafa, H. Yeek-Chia, L. Baloo, T. S. B. Abd Manan and M. O. Saeed, Cr (VI) adsorption from aqueous solution by an agricultural waste based carbon, *RSC Adv.*, 2016, **6**, 56365–56374.

69 M. Solgi, T. Najib, S. Ahmadnejad and B. Nasernejad, Synthesis and characterization of novel activated carbon from Medlar seed for chromium removal: experimental analysis and modeling with artificial neural network and support vector regression, *Resour.-Effic. Technol.*, 2017, **3**, 236–248.

70 K. Singh, J. K. Arora, T. J. M. Sinha and S. Srivastava, Functionalization of nanocrystalline cellulose for decontamination of Cr (III) and Cr (VI) from aqueous system: computational modeling approach, *Clean Technol. Environ. Policy*, 2014, **16**, 1179–1191.

71 V. Singh, J. Singh and V. Mishra, Development of a cost-effective, recyclable and viable metal ion doped adsorbent for simultaneous adsorption and reduction of toxic Cr (VI) ions, *J. Environ. Chem. Eng.*, 2021, **9**, 105124.

72 C. Sutherland, A. Marcano and B. Chittoo, Artificial neural network-genetic algorithm prediction of heavy metal removal using a novel plant-based biosorbent banana floret: kinetic, equilibrium, thermodynamics and desorption studies, in *Desalination Water Treat.*, IntechOpen, 2018, pp. 385–411.

73 K. Yadav, M. Raphi and S. Jagadevan, Adsorption of copper (II) on chemically modified biochar: a single-stage batch adsorber design and predictive modeling through artificial neural network, *Biomass Convers. Biorefinery*, 2021, 1–16.

74 T. Khan, M. R. U. Mustafa, M. H. Isa, T. S. B. A. Manan, Y.-C. Ho, J.-W. Lim and N. Z. Yusof, Artificial neural network (ANN) for modelling adsorption of lead (Pb (II)) from aqueous solution, *Water. Air. Soil Pollut.*, 2017, **228**, 1–15.

75 M. Ashrafi, H. Borzuie, G. Bagherian, M. A. Chamjangali and H. Nikoofard, Artificial neural network and multiple linear regression for modeling sorption of Pb2+ ions from aqueous solutions onto modified walnut shell, *Sep. Sci. Technol.*, 2020, **55**, 222–233.

76 S. Ullah, M. A. Assiri, A. G. Al-Sehemi, M. A. Bustam, M. Sagir, F. A. Abdulkareem, M. R. Raza, M. Ayoub and A. Irfan, Characteristically insights, artificial neural network (ANN), equilibrium, and kinetic studies of Pb (II) ion adsorption on rice husks treated with nitric acid, *Int. J. Environ. Res.*, 2020, **14**, 43–60.

77 M. Pazouki, M. Zabihi, J. Shayegan and M. H. Fatehi, Mercury ion adsorption on AC@Fe3O4-NH2-COOH from saline solutions: experimental studies and artificial neural network modeling, *Korean J. Chem. Eng.*, 2018, **35**, 671–683.

78 B. R. Broujeni, A. Nilchi and F. Azadi, Adsorption modeling and optimization of thorium (IV) ion from aqueous solution using chitosan/TiO2 nanocomposite: application of artificial neural network and genetic algorithm, *Environ. Nanotechnol. Monit. Manag.*, 2021, **15**, 100400.

79 H. Heshmati, M. Torab-Mostaedi, H. Ghanadzadeh Gilani and A. Heydari, Kinetic, isotherm, and thermodynamic investigations of uranium (VI) adsorption on synthesized ion-exchange chelating resin and prediction with an artificial neural network, *Desalination Water Treat.*, 2015, **55**, 1076–1087.

80 S. Rebouh, M. Bouhedda and S. Hanini, Neuro-fuzzy modeling of Cu (II) and Cr (VI) adsorption from aqueous solution by wheat straw, *Desalination Water Treat.*, 2016, **57**, 6515–6530.

81 S. Varshney, P. Jain, J. K. Arora and S. Srivastava, Process development for the removal of toxic metals by functionalized wood pulp: kinetic, thermodynamic, and computational modeling approach, *Clean Technol. Environ. Policy*, 2016, **18**, 2613–2623.

82 F. Brouers and T. J. Al-Musawi, On the optimal use of isotherm models for the characterization of biosorption of lead onto algae, *J. Mol. Liq.*, 2015, **212**, 46–51, DOI: 10.1016/j.molliq.2015.08.054.

83 A. H. Hamidian, S. Esfandeh, Y. Zhang and M. Yang, Simulation and optimization of nanomaterials application for heavy metal removal from aqueous solutions, *Inorg. Nano-Met. Chem.*, 2019, **49**, 217–230.

84 A. Ronda, M. A. Martín-Lara, A. I. Almendros, A. Pérez and G. Blázquez, Comparison of two models for the biosorption of Pb (II) using untreated and chemically treated olive stone: experimental design methodology and adaptive neural fuzzy inference system (ANFIS), *J. Taiwan Inst. Chem. Eng.*, 2015, **54**, 45–56.

85 P. L. Narayana, A. K. Maurya, X.-S. Wang, M. R. Harsha, O. Srikanth, A. A. Alnuaim, W. A. Hatamleh, A. A. Hatamleh, K. K. Cho and U. M. Reddy, Artificial neural networks modeling for lead removal from aqueous solutions using iron oxide nanocomposites from bio-waste mass, *Environ. Res.*, 2021, 111370.

86 Y. J. Wong, S. K. Arumugasamy, C. H. Chung, A. Selvarajoo and V. Sethu, Comparative study of artificial neural network (ANN), adaptive neuro-fuzzy inference system (ANFIS) and multiple linear regression (MLR) for modeling of Cu (II) adsorption from aqueous solution using biochar derived from rambutan (Nephelium lappaceum) peel, *Environ. Monit. Assess.*, 2020, **192**, 1–20.

87 P. J. Braspenning, F. Thuijsman and A. J. M. M. Weijters, *Artificial Neural Networks: an Introduction to ANN Theory and Practice*, Springer Science & Business Media, 1995.

88 A. T. Goh, Back-propagation neural networks for modeling complex systems, *Artif. Intell. Eng.*, 1995, **9**, 143–151.

89 P. P. Van Der Smagt, Minimisation methods for training feedforward neural networks, *Neural Network.*, 1994, **7**, 1–11.

90 Z. Wang, H. Zhang, J. Ren, X. Lin, T. Han, J. Liu and J. Li, Predicting adsorption ability of adsorbents at arbitrary

sites for pollutants using deep transfer learning, *Npj Comput. Mater.*, 2021, **7**, 1–9, DOI: **10.1038/s41524-021-00494-9**.

91 M. Fawzy, M. Nasr, H. Nagy and S. Helmi, Artificial intelligence and regression analysis for Cd (II) ion biosorption from aqueous solution by Gossypium barbadense waste, *Environ. Sci. Pollut. Res.*, 2018, **25**, 5875–5888.

92 D. I. Mendoza-Castillo, N. Villalobos-Ortega, A. Bonilla-Petriciolet and J. C. Tapia-Picazo, Neural network modeling of heavy metal sorption on lignocellulosic biomasses: effect of metallic ion properties and sorbent characteristics, *Ind. Eng. Chem. Res.*, 2015, **54**, 443–453.

93 A. A. Prabhu, S. Chityala, D. Jayachandran, N. N. Deshavath and V. D. Veeranki, A two step optimization approach for maximizing biosorption of hexavalent chromium ions (Cr (VI)) using alginate immobilized Sargassum sp in a packed bed column, *Sep. Sci. Technol.*, 2021, **56**, 90–106.

94 L. T. Popoola, Nano-magnetic walnut shell-rice husk for Cd (II) sorption: design and optimization using artificial intelligence and design expert, *Heliyon*, 2019, **5**, e02381.

95 F. Kartal and U. Özveren, An improved machine learning approach to estimate hemicellulose, cellulose, and lignin in biomass, *Carbohydr. Polym. Technol. Appl.*, 2021, **2**, 100148.

96 H. A. Hamid, Y. Jenidi, W. Thielemans, C. Somerfield and R. L. Gomes, Predicting the capability of carboxylated cellulose nanowhiskers for the remediation of copper from water using response surface methodology (RSM) and artificial neural network (ANN) models, *Ind. Crops Prod.*, 2016, **93**, 108–120.

97 D. Krishna, G. S. Kumar and D. R. P. Raju, Optimization of Process Parameters for the Removal of Chromium (VI) from Waste Water Using Mixed Adsorbent, *Int. J. Appl. Sci. Eng.*, 2019, **16**, 187–200.

98 M. Shanmugaprakash, S. Venkatachalam, K. Rajendran and A. Pugazhendhi, Biosorptive removal of Zn (II) ions by Pongamia oil cake (Pongamia pinnata) in batch and fixed-bed column studies using response surface methodology and artificial neural network, *J. Environ. Manage.*, 2018, **227**, 216–228.

99 E. Allahkarami, A. Igder, A. Fazlavi and B. Rezai, Prediction of Co (II) and Ni (II) ions removal from wastewater using artificial neural network and multiple regression models, *Physicochem. Probl. Miner. Process.*, 2017, **53**, 1105–1118.

100 M. Banerjee, N. Bar and S. K. Das, Cu (II) removal from aqueous solution using the walnut shell: adsorption study, regeneration study, plant scale-up design, economic feasibility, statistical, and GA-ANN modeling, *Int. J. Environ. Res.*, 2021, **15**, 875–891.

101 P. Moradi, S. Hayati and T. Ghahrizadeh, Modeling and optimization of lead and cobalt biosorption from water with Rafsanjan pistachio shell, using experiment based models of ANN and GP, and the grey wolf optimizer, *Chemom. Intell. Lab. Syst.*, 2020, **202**, 104041.

102 J. A. Rodríguez-Romero, D. I. Mendoza-Castillo, H. E. Reynel-Ávila, D. A. de Haro-Del Rio, L. M. González-Rodríguez, A. Bonilla-Petriciolet, C. J. Duran-Valle and K. I. Camacho-Aguilar, Preparation of a new adsorbent for the removal of arsenic and its simulation with artificial neural network-based adsorption models, *J. Environ. Chem. Eng.*, 2020, **8**, 103928.

103 X. Zheng and H. Nguyen, A novel artificial intelligent model for predicting water treatment efficiency of various biochar systems based on artificial neural network and queuing search algorithm, *Chemosphere*, 2022, **287**, 132251.

104 Q. Dai and N. Liu, Alleviating the problem of local minima in backpropagation through competitive learning, *Neurocomputing*, 2012, **94**, 152–158.

105 H.-X. Huang, J.-C. Li and C.-L. Xiao, A proposed iteration optimization approach integrating backpropagation neural network with genetic algorithm, *Expert Syst. Appl.*, 2015, **42**, 146–155.

106 G. Dhiman, SSC: a hybrid nature-inspired meta-heuristic optimization algorithm for engineering applications, *Knowl. Base Syst.*, 2021, **222**, 106926.

107 B. Ke, H. Nguyen, X.-N. Bui, H.-B. Bui, Y. Choi, J. Zhou, H. Moayedi, R. Costache and T. Nguyen-Trang, Predicting the sorption efficiency of heavy metal based on the biochar characteristics, metal sources, and environmental conditions using various novel hybrid machine learning models, *Chemosphere*, 2021, **276**, 130204.

108 M. Khishe and M. R. Mosavi, Chimp optimization algorithm, *Expert Syst. Appl.*, 2020, **149**, 113338.

109 M. Shehab, A. T. Khader, M. Laouchedi and O. A. Alomari, Hybridizing cuckoo search algorithm with bat algorithm for global numerical optimization, *J. Supercomput.*, 2019, **75**, 2395–2422.

110 A. Ahmad, M. Sulaiman, A. Alhindi and A. J. Aljohani, Analysis of temperature profiles in longitudinal fin designs by a novel neuroevolutionary approach, *IEEE Access*, 2020, **8**, 113285–113308.

111 J. M. Chaharmahali and M. Shabanzadeh, A Machine Learning-Assisted Clustering Engine to Enhance the Accuracy of Hourly Load Forecasting, in *2020 10th Smart Grid Conf. SGC*, IEEE, 2020, pp. 1–6.

112 M. Farzaneh-Gord, B. Mohseni-Gharyehsafa, A. Ebrahimi-Moghadam, A. Jabari-Moghadam, A. Toikka and I. Zvereva, Precise calculation of natural gas sound speed using neural networks: an application in flow meter calibration, *Flow Meas. Instrum.*, 2018, **64**, 90–103.

113 M. S. Saad, A. Mohd Nor, I. Abd Rahim, M. A. Syahruddin and I. Z. Mat Darus, Optimization of FDM process parameters to minimize surface roughness with integrated artificial neural network model and symbiotic organism search, *Neural Comput. Appl.*, 2022, 1–17.

114 S. Mirjalili, S. M. Mirjalili and A. Lewis, Grey wolf optimizer, *Adv. Eng. Softw.*, 2014, **69**, 46–61.

115 J.-S. Wang and S.-X. Li, An Improved Grey Wolf Optimizer Based on Differential Evolution and Elimination Mechanism, *Sci. Rep.*, 2019, **9**, 7181, DOI: **10.1038/s41598-019-43546-3**.

116 S. Nosratabadi, K. Szell, B. Beszedes, F. Imre, S. Ardabili and A. Mosavi, Comparative Analysis of ANN-ICA and

ANN-GWO for Crop Yield Prediction, in *2020 RIVF Int. Conf. Comput. Commun. Technol. RIVF*, IEEE, 2020, pp. 1–5.

117 S. Ardabili, A. Mosavi, S. S. Band and A. R. Varkonyi-Koczy, Coronavirus disease (COVID-19) global prediction using hybrid artificial intelligence method of ANN trained with Grey Wolf optimizer, in *2020 IEEE 3rd Int. Conf. Workshop Óbuda Electr. Power Eng. CANDO-EPE*, IEEE, 2020, pp. 000251–000254.

118 A. Seifi and F. Soroush, Pan evaporation estimation and derivation of explicit optimized equations by novel hybrid meta-heuristic ANN based methods in different climates of Iran, *Comput. Electron. Agric.*, 2020, **173**, 105418, DOI: **10.1016/j.compag.2020.105418**.

119 A. Sharma and U. Tyagi, A Hybrid Approach of ANN-GWO Technique for Intrusion Detection, in *2021 Int. Conf. Recent Trends Electron. Inf. Commun. Technol. RTEICT*, 2021, pp. 467–472, DOI: **10.1109/RTEICT52294.2021.9573800**.

120 B. Yuce and Y. Rezgui, An ANN-GA semantic rule-based system to reduce the gap between predicted and actual energy consumption in buildings, *IEEE Trans. Autom. Sci. Eng.*, 2015, **14**, 1351–1363.

121 M. Akgül, Ö. E. Sönmez and T. Özcan, Diagnosis of heart disease using an intelligent method: a hybrid ANN–GA approach, in *Int. Conf. Intell. Fuzzy Syst.*, Springer, 2019, pp. 1250–1257.

122 S. Bahrami, F. Doulati Ardejani and E. Baafi, Application of artificial neural network coupled with genetic algorithm and simulated annealing to solve groundwater inflow problem to an advancing open pit mine, *J. Hydrol.*, 2016, **536**, 471–484, DOI: **10.1016/j.jhydrol.2016.03.002**.

123 K. S. Sangwan, S. Saxena and G. Kant, Optimization of machining parameters to minimize surface roughness using integrated ANN-GA approach, *Procedia Cirp*, 2015, **29**, 305–310.

124 A. A. Kulaksız and R. Akkaya, A genetic algorithm optimized ANN-based MPPT algorithm for a stand-alone PV system with induction motor drive, *Sol. Energy*, 2012, **86**, 2366–2375.

125 X. Lü, Y. Wu, J. Lian, Y. Zhang, C. Chen, P. Wang and L. Meng, Energy management of hybrid electric vehicles: a review of energy optimization of fuel cell hybrid power system based on genetic algorithm, *Energy Convers. Manag.*, 2020, **205**, 112474.

126 J. Zhang, M. Xiao, L. Gao and Q. Pan, Queuing search algorithm: a novel metaheuristic algorithm for solving engineering optimization problems, *Appl. Math. Model.*, 2018, **63**, 464–490.

127 S. Gupta, H. Abderazek, B. S. Yıldız, A. R. Yildiz, S. Mirjalili and S. M. Sait, Comparison of metaheuristic optimization algorithms for solving constrained mechanical design optimization problems, *Expert Syst. Appl.*, 2021, **183**, 115351.

128 J. Zhan, M. Fard and R. Jazar, A CAD-FEM-QSA integration technique for determining the time-varying meshing stiffness of gear pairs, *Measurement*, 2017, **100**, 139–149, DOI: **10.1016/j.measurement.2016.12.056**.

129 M. Nasr, A. E. D. Mahmoud, M. Fawzy and A. Radwan, Artificial intelligence modeling of cadmium (II) biosorption using rice straw, *Appl. Water Sci.*, 2017, **7**, 823–831.

130 I. M. El-Hasnony, S. I. Barakat and R. R. Mostafa, Optimized ANFIS model using hybrid metaheuristic algorithms for Parkinson's disease prediction in IoT environment, *IEEE Access*, 2020, **8**, 119252–119270.

131 Z. Yun, Z. Quan, S. Caixin, L. Shaolan, L. Yuming and S. Yang, RBF neural network and ANFIS-based short-term load forecasting approach in real-time price environment, *IEEE Trans. Power Syst.*, 2008, **23**, 853–858.

132 M. Şahin and R. Erol, A comparative study of neural networks and ANFIS for forecasting attendance rate of soccer games, *Math. Comput. Appl.*, 2017, **22**, 43.

133 P. Srisaeng and G. Baxter, Application of an ANFIS to Estimate Kansai International Airport's International Air Passenger Demand, *J. Aviat.*, 2022, **6**, 87–92.

134 B. M. Wilamowski, Neural network architectures and learning algorithms, *IEEE Ind. Electron. Mag.*, 2009, **3**, 56–63.

135 E. Siregar, H. Mawengkang, E. B. Nababan and A. Wanto, Analysis of Backpropagation Method with Sigmoid Bipolar and Linear Function in Prediction of Population Growth, in *J. Phys. Conf. Ser.*, IOP Publishing, 2019, p. 012023.

136 M. A. Mercioni and S. Holban, The most used activation functions: Classic versus current, in *2020 Int. Conf. Dev. Appl. Syst.*, DAS, IEEE, 2020, pp. 141–145.

137 B. K. Nath, C. Chaliha and E. Kalita, Iron oxide Permeated Mesoporous rice-husk nanobiochar (IPMN) mediated removal of dissolved arsenic (As): chemometric modelling and adsorption dynamics, *J. Environ. Manage.*, 2019, **246**, 397–409.

138 D. Ranjan, D. Mishra and S. H. Hasan, Bioadsorption of arsenic: an artificial neural networks and response surface methodological approach, *Ind. Eng. Chem. Res.*, 2011, **50**, 9852–9863.

139 M. Shanmugaprakash and V. Sivakumar, Development of experimental design approach and ANN-based models for determination of Cr (VI) ions uptake rate from aqueous solution onto the solid biodiesel waste residue, *Bioresour. Technol.*, 2013, **148**, 550–559.

140 D. Whitley, S. Rana, J. Dzubera and K. E. Mathias, Evaluating evolutionary algorithms, *Artif. Intell.*, 1996, **85**, 245–276.

141 K. Yetilmezsoy and S. Demirel, Artificial neural network (ANN) approach for modeling of Pb (II) adsorption from aqueous solution by Antep pistachio (Pistacia Vera L.) shells, *J. Hazard. Mater.*, 2008, **153**, 1288–1300.

142 N. Prakash, S. A. Manikandan, L. Govindarajan and V. Vijayagopal, Prediction of biosorption efficiency for the removal of copper (II) using artificial neural networks, *J. Hazard. Mater.*, 2008, **152**, 1268–1275.

143 A. K. Giri, R. K. Patel and S. S. Mahapatra, Artificial neural network (ANN) approach for modelling of arsenic (III)

biosorption from aqueous solution by living cells of Bacillus cereus biomass, *Chem. Eng. J.*, 2011, **178**, 15–25.
144 A. Kardam, K. R. Raj, J. K. Arora and S. Srivastava, Artificial neural network modeling for biosorption of Pb (II) ions on nanocellulose fibers, *Bionanoscience*, 2012, **2**, 153–160.
145 K. R. Raj, A. Kardam, J. K. Arora and S. Srivastava, An application of ANN modeling on the biosorption of arsenic, *Waste Biomass Valorization*, 2013, **4**, 401–407.
146 B. Singha, N. Bar and S. K. Das, The use of artificial neural networks (ANN) for modeling of adsorption of Cr (VI) ions, *Desalination Water Treat.*, 2014, **52**, 415–425.
147 B. Singha, N. Bar and S. K. Das, The use of artificial neural network (ANN) for modeling of Pb (II) adsorption in batch process, *J. Mol. Liq.*, 2015, **211**, 228–232.
148 M. S. Podder and C. B. Majumder, The use of artificial neural network for modelling of phycoremediation of toxic elements As (III) and As (V) from wastewater using Botryococcus braunii, *Spectrochim. Acta Mol. Biomol. Spectrosc.*, 2016, **155**, 130–145.
149 H. Esfandian, M. Parvini, B. Khoshandam and A. Samadi-Maybodi, Artificial neural network (ANN) technique for modeling the mercury adsorption from aqueous solution using Sargassum Bevanom algae, *Desalination Water Treat.*, 2016, **57**, 17206–17219.
150 S. Nag, A. Mondal, N. Bar and S. K. Das, Biosorption of chromium (VI) from aqueous solutions and ANN modelling, *Environ. Sci. Pollut. Res.*, 2017, **24**, 18817–18835.
151 M. Banerjee, N. Bar, R. K. Basu and S. K. Das, Comparative study of adsorptive removal of Cr (VI) ion from aqueous solution in fixed bed column by peanut shell and almond shell using empirical models and ANN, *Environ. Sci. Pollut. Res.*, 2017, **24**, 10604–10620.
152 R. S. Kiran, G. M. Madhu, S. V. Satyanarayana, P. Kalpana and G. S. Rangaiah, Applications of Box–Behnken experimental design coupled with artificial neural networks for biosorption of low concentrations of cadmium using Spirulina (Arthrospira) spp, *Resour.-Effic. Technol.*, 2017, **3**, 113–123.
153 A. Kardam, K. R. Raj, J. K. Arora, M. M. Srivastava and S. Srivastava, Artificial neural network modeling for sorption of cadmium from aqueous system by shelled Moringa oleifera seed powder as an agricultural waste, *J. Water Resour. Prot.*, 2010, **2**, 339.
154 L. T. Popoola, Nano-magnetic walnut shell-rice husk for Cd (II) sorption: design and optimization using artificial intelligence and design expert, *Heliyon*, 2019, **5**, e02381.
155 M. Fawzy, M. Nasr, S. Adel and S. Helmi, Regression model, artificial neural network, and cost estimation for biosorption of Ni (II)-ions from aqueous solutions by Potamogeton pectinatus, *Int. J. Phytoremediation*, 2018, **20**, 321–329.
156 D. Krishna and R. P. Sree, Artificial Neural Network (ANN) Approach for modeling chromium (VI) adsorption from aqueous solution using a Borasus Flabellifer coir powder, *Int. J. Appl. Sci. Eng.*, 2014, **12**, 177–192.
157 D. Krishna, G. S. Kumar and D. R. P. Raju, Optimization of Process Parameters for the Removal of Chromium (VI) from Waste Water Using Mixed Adsorbent, *Int. J. Appl. Sci. Eng.*, 2019, **16**, 187–200.
158 N. Parveen, S. Zaidi and M. Danish, Development of SVR-based model and comparative analysis with MLR and ANN models for predicting the sorption capacity of Cr (VI), *Process Saf. Environ. Prot.*, 2017, **107**, 428–437.
159 W. A. H. Altowayti, H. A. Algaifi, S. A. Bakar and S. Shahir, The adsorptive removal of As (III) using biomass of arsenic resistant Bacillus thuringiensis strain WS3: characteristics and modelling studies, *Ecotoxicol. Environ. Saf.*, 2019, **172**, 176–185.
160 R. Beigzadeh and S. O. Rastegar, Assessment of Cr (VI) Biosorption from Aqueous Solution by Artificial Intelligence, *Chem. Methodol.*, 2020, **4**, 181–190.
161 E. Oguz and M. Ersoy, Removal of Cu2+ from aqueous solution by adsorption in a fixed bed column and Neural Network Modelling, *Chem. Eng. J.*, 2010, **164**, 56–62.
162 N. G. Turan, B. Mesci and O. Ozgonenel, Artificial neural network (ANN) approach for modeling Zn (II) adsorption from leachate using a new biosorbent, *Chem. Eng. J.*, 2011, **173**, 98–105.
163 D. Bingöl, M. Hercan, S. Elevli and E. Kılıç, Comparison of the results of response surface methodology and artificial neural network for the biosorption of lead using black cumin, *Bioresour. Technol.*, 2012, **112**, 111–115.
164 M. F. Ahmad, S. Haydar, A. A. Bhatti and A. J. Bari, Application of artificial neural network for the prediction of biosorption capacity of immobilized Bacillus subtilis for the removal of cadmium ions from aqueous solution, *Biochem. Eng. J.*, 2014, **84**, 83–90.
165 U. Yurtsever, M. Yurtsever, İ. A. Şengil and N. Kıratlı Yılmazçoban, Fast artificial neural network (FANN) modeling of Cd (II) ions removal by valonia resin, *Desalination Water Treat.*, 2015, **56**, 83–96.
166 S. Yildiz, Artificial neural network (ANN) approach for modeling Zn (II) adsorption in batch process, *Korean J. Chem. Eng.*, 2017, **34**, 2423–2434.
167 F. Rahimpour, T. Shojaeimehr and M. Sadeghi, Biosorption of Pb (II) using Gundelia tournefortii: kinetics, equilibrium, and thermodynamics, *Sep. Sci. Technol.*, 2017, **52**, 596–607.
168 S. G. Shandi, F. D. Ardejani and F. Sharifi, Assessment of Cu (II) removal from an aqueous solution by raw Gundelia tournefortii as a new low-cost biosorbent: experiments and modelling, *Chin. J. Chem. Eng.*, 2019, **27**, 1945–1955.
169 M. R. Fagundes-Klen, P. Ferri, T. D. Martins, C. R. G. Tavares and E. A. Silva, Equilibrium study of the binary mixture of cadmium–zinc ions biosorption by the Sargassum filipendula species using adsorption isotherms models and neural network, *Biochem. Eng. J.*, 2007, **34**, 136–146.
170 D. Bingöl, M. Inal and S. Çetintaş, Evaluation of copper biosorption onto date palm (Phoenix dactylifera L.) seeds with MLR and ANFIS models, *Ind. Eng. Chem. Res.*, 2013, **52**, 4429–4435.
171 S. A. Jafari and S. Cheraghi, Mercury removal from aqueous solution by dried biomass of indigenous Vibrio

parahaemolyticus PG02: kinetic, equilibrium, and thermodynamic studies, *Int. Biodeterior. Biodegrad.*, 2014, **92**, 12–19.

172 M. Fawzy, M. Nasr, S. Adel, H. Nagy and S. Helmi, Environmental approach and artificial intelligence for Ni (II) and Cd (II) biosorption from aqueous solution using Typha domingensis biomass, *Ecol. Eng.*, 2016, **95**, 743–752.

173 M. Fawzy, M. Nasr, A. Abdel-Gaber and S. Fadly, Biosorption of Cr (VI) from aqueous solution using agricultural wastes, with artificial intelligence approach, *Sep. Sci. Technol.*, 2016, **51**, 416–426.

174 S. Nag, N. Bar and S. K. Das, Cr (VI) removal from aqueous solution using green adsorbents in continuous bed column–statistical and GA-ANN hybrid modelling, *Chem. Eng. Sci.*, 2020, **226**, 115904.

175 B. R. Broujeni, A. Nilchi and F. Azadi, Adsorption modeling and optimization of thorium (IV) ion from aqueous solution using chitosan/TiO2 nanocomposite: application of artificial neural network and genetic algorithm, *Environ. Nanotechnol. Monit. Manag.*, 2021, **15**, 100400.

176 A. A. Prabhu, S. Chityala, D. Jayachandran, N. N. Deshavath and V. D. Veeranki, A two step optimization approach for maximizing biosorption of hexavalent chromium ions (Cr (VI)) using alginate immobilized Sargassum sp in a packed bed column, *Sep. Sci. Technol.*, 2021, **56**, 90–106.

177 M. Khajeh and E. Jahanbin, Application of cuckoo optimization algorithm–artificial neural network method of zinc oxide nanoparticles–chitosan for extraction of uranium from water samples, *Chemom. Intell. Lab. Syst.*, 2014, **135**, 70–75.

178 A. M. Abu El-Soad, G. Lazzara, M. O. Abd El-Magied, G. Cavallaro, J. S. Al-Otaibi, M. I. Sayyed and E. G. Kovaleva, Chitosan Functionalized with Carboxyl Groups as a Recyclable Biomaterial for the Adsorption of Cu (II) and Zn (II) Ions in Aqueous Media, *Int. J. Mol. Sci.*, 2022, **23**, 2396.

179 A. Çelekli, A. I. Al-Nuaimi and H. Bozkurt, Adsorption kinetic and isotherms of Reactive Red 120 on Moringa oleifera seed as an eco-friendly process, *J. Mol. Struct.*, 2019, **1195**, 168–178.

180 S. Narayanasamy, V. Sundaram, T. Sundaram and D.-V. N. Vo, Biosorptive ascendency of plant based biosorbents in removing hexavalent chromium from aqueous solutions–Insights into isotherm and kinetic studies, *Environ. Res.*, 2022, **210**, 112902.

181 N. A. Negm, M. G. Abd El Wahed, A. R. A. Hassan and M. T. Abou Kana, Feasibility of metal adsorption using brown algae and fungi: effect of biosorbents structure on adsorption isotherm and kinetics, *J. Mol. Liq.*, 2018, **264**, 292–305.

182 M. G. Alalm and M. Nasr, Artificial intelligence, regression model, and cost estimation for removal of chlorothalonil pesticide by activated carbon prepared from casuarina charcoal, *Sustain. Environ. Res.*, 2018, **28**, 101–110.

183 B. G. Saucedo-Delgado, D. A. De Haro-Del Rio, L. M. González-Rodríguez, H. E. Reynel-Ávila, D. I. Mendoza-Castillo, A. Bonilla-Petriciolet and J. R. de la Rosa, Fluoride adsorption from aqueous solution using a protonated clinoptilolite and its modeling with artificial neural network-based equations, *J. Fluorine Chem.*, 2017, **204**, 98–106.

184 R. Tovar-Gómez, M. R. Moreno-Virgen, J. A. Dena-Aguilar, V. Hernández-Montoya, A. Bonilla-Petriciolet and M. A. Montes-Morán, Modeling of fixed-bed adsorption of fluoride on bone char using a hybrid neural network approach, *Chem. Eng. J.*, 2013, **228**, 1098–1109.

185 S. Verma and A. Kuila, Bioremediation of heavy metals by microbial process, *Environ. Technol. Innovat.*, 2019, **14**, 100369.

186 M. S. Netto, J. S. Oliveira, N. P. Salau and G. L. Dotto, Analysis of adsorption isotherms of Ag+, Co+2, and Cu+2 onto zeolites using computational intelligence models, *J. Environ. Chem. Eng.*, 2021, **9**, 104960.

187 M. Dolatabadi, M. Mehrabpour, M. Esfandyari, H. Alidadi and M. Davoudi, Modeling of simultaneous adsorption of dye and metal ion by sawdust from aqueous solution using of ANN and ANFIS, *Chemom. Intell. Lab. Syst.*, 2018, **181**, 72–78, DOI: **10.1016/j.chemolab.2018.07.012**.

188 D. I. Mendoza-Castillo, H. E. Reynel-Ávila, F. J. Sánchez-Ruiz, R. Trejo-Valencia, J. E. Jaime-Leal and A. Bonilla-Petriciolet, Insights and pitfalls of artificial neural network modeling of competitive multi-metallic adsorption data, *J. Mol. Liq.*, 2018, **251**, 15–27.

189 A. Gopinath, B. G. Retnam, A. Muthukkumaran and K. Aravamudan, Swift, versatile and a rigorous kinetic model based artificial neural network surrogate for single and multicomponent batch adsorption processes, *J. Mol. Liq.*, 2020, **297**, 111888.

190 J. D. Olden, M. K. Joy and R. G. Death, An accurate comparison of methods for quantifying variable importance in artificial neural networks using simulated data, *Ecol. Model.*, 2004, **178**, 389–397.

191 A. K. Abraham, W. Krzyzanski and D. E. Mager, Partial derivative—based sensitivity analysis of models describing target-mediated drug disposition, *AAPS J.*, 2007, **9**, E181–E189.

192 M. Gevrey, I. Dimopoulos and S. Lek, Two-way interaction of input variables in the sensitivity analysis of neural network models, *Ecol. Model.*, 2006, **195**, 43–50.

193 P. K. Srivastava, M. Gupta, U. Singh, R. Prasad, P. C. Pandey, A. S. Raghubanshi and G. P. Petropoulos, Sensitivity analysis of artificial neural network for chlorophyll prediction using hyperspectral data, *Environ. Dev. Sustain.*, 2021, **23**, 5504–5519.

194 M. Gevrey, I. Dimopoulos and S. Lek, Review and comparison of methods to study the contribution of variables in artificial neural network models, *Ecol. Model.*, 2003, **160**, 249–264.

195 K. Zeng, K. Hachem, M. Kuznetsova, S. Chupradit, C.-H. Su, H. C. Nguyen and A. S. El-Shafay, Molecular dynamic simulation and artificial intelligence of lead ions removal from aqueous solution using magnetic-ash-graphene oxide nanocomposite, *J. Mol. Liq.*, 2022, **347**, 118290.

196 J. H. Montoya and K. A. Persson, A high-throughput framework for determining adsorption energies on solid surfaces, *Npj Comput. Mater.*, 2017, **3**, 1–4, DOI: **10.1038/s41524-017-0017-z**.

197 B. Li, X. Li, W. Gao and Q. Jiang, An effective scheme to determine surface energy and its relation with adsorption energy, *Acta Mater.*, 2021, **212**, 116895, DOI: **10.1016/j.actamat.2021.116895**.

198 Y. Zhu, B. Luo, C. Sun, J. Liu, H. Sun, Y. Li and Y. Han, Density functional theory study of α-bromolauric acid adsorption on the α-quartz (1 0 1) surface, *Miner. Eng.*, 2016, **92**, 72–77.

199 V. R. Pavithra, T. Daniel Thangadurai, G. Manonmani, K. Senthilkumar, D. Nataraj, J. Jiya, K. Nandakumar and S. Thomas, Investigation on surface interaction between graphene nanobuds and cerium(III) via fluorescence excimer, theoretical, real water sample, and bioimaging studies, *Mater. Chem. Phys.*, 2021, **264**, 124453, DOI: **10.1016/j.matchemphys.2021.124453**.

200 M. A. Hubbe, Insisting upon meaningful results from adsorption experiments, *Sep. Purif. Rev.*, 2022, **51**, 212–225.

201 D. Q. Gbadago, J. Moon, M. Kim and S. Hwang, A unified framework for the mathematical modelling, predictive analysis, and optimization of reaction systems using computational fluid dynamics, deep neural network and genetic algorithm: a case of butadiene synthesis, *Chem. Eng. J.*, 2021, **409**, 128163.

202 L. T. Yogarathinam, K. Velswamy, A. Gangasalam, A. F. Ismail, P. S. Goh, M. N. Subramaniam, M. S. Narayana, N. Yaacob and M. S. Abdullah, Parametric analysis of lignocellulosic ultrafiltration in lab scale cross flow module using pore blocking and artificial neural network model, *Chemosphere*, 2022, **286**, 131822.

203 L. I. Weidong, M. K. Suhayb, L. Thangavelu, H. A. Marhoon, I. Pustokhina, U. F. Alqsair, A. S. El-Shafay and M. Alashwal, Implementation of AdaBoost and genetic algorithm machine learning models in prediction of adsorption capacity of nanocomposite materials, *J. Mol. Liq.*, 2022, **350**, 118527.

204 M. Fan, J. Hu, R. Cao, K. Xiong and X. Wei, Modeling and prediction of copper removal from aqueous solutions by nZVI/rGO magnetic nanocomposites using ANN-GA and ANN-PSO, *Sci. Rep.*, 2017, **7**, 1–14.

205 W. Wang, X. Wu and S. Long, Optimizing the Methylene Blue Removal from Aqueous Solution Using Pomelo Peel Based Biochar Assisted by RSM and ANN-PSO, *Pol. J. Environ. Stud.*, 2022, **31**, 329–346.

206 S. K. Bhagat, T. M. Tung and Z. M. Yaseen, Development of artificial intelligence for modeling wastewater heavy metal removal: state of the art, application assessment and possible future research, *J. Cleaner Prod.*, 2020, **250**, 119473.

207 G. Alam, I. Ihsanullah, M. Naushad and M. Sillanpää, Applications of artificial intelligence in water treatment for optimization and automation of adsorption processes: recent advances and prospects, *Chem. Eng. J.*, 2022, **427**, 130011.

208 H. E. Reynel-Ávila, I. A. Aguayo-Villarreal, L. L. Diaz-Muñoz, J. Moreno-Pérez, F. J. Sánchez-Ruiz, C. K. Rojas-Mayorga, D. I. Mendoza-Castillo and A. Bonilla-Petriciolet, A Review of the Modeling of Adsorption of Organic and Inorganic Pollutants from Water Using Artificial Neural Networks, *Adsorpt. Sci. Technol.*, 2022, **2022**.

209 Z. M. Yaseen, An insight into machine learning models era in simulating soil, water bodies and adsorption heavy metals: review, challenges and solutions, *Chemosphere*, 2021, **277**, 130126.

210 S. P. G. Zaferani, M. R. S. Emami, M. K. Amiri and E. Binaeian, Optimization of the removal Pb (II) and its Gibbs free energy by thiosemicarbazide modified chitosan using RSM and ANN modeling, *Int. J. Biol. Macromol.*, 2019, **139**, 307–319.

211 A. Rodríguez-Romero, D. I. Mendoza-Castillo, H. E. Reynel-Ávila, D. A. de Haro-Del Rio, L. M. González-Rodríguez, A. Bonilla-Petriciolet, C. J. Duran-Valle and K. I. Camacho-Aguilar, Preparation of a new adsorbent for the removal of arsenic and its simulation with artificial neural network-based adsorption models, *J. Environ. Chem. Eng.*, 2020, **8**, 103928.

212 P. S. Pauletto, G. L. Dotto and N. P. Salau, Optimal artificial neural network design for simultaneous modeling of multicomponent adsorption, *J. Mol. Liq.*, 2020, **320**, 114418.

213 C. Escobar, C. Soto-Salazar and M. I. Toral, Optimization of the electrocoagulation process for the removal of copper, lead and cadmium in natural waters and simulated wastewater, *J. Environ. Manage.*, 2006, **81**, 384–391.

214 Y. Wang, S. Wang, T. Xie and J. Cao, Activated carbon derived from waste tangerine seed for the high-performance adsorption of carbamate pesticides from water and plant, *Bioresour. Technol.*, 2020, **316**, 123929.

215 J. L. Fagundez, M. S. Netto, G. L. Dotto and N. P. Salau, A new method of developing ANN-isotherm hybrid models for the determination of thermodynamic parameters in the adsorption of ions Ag^{+}, Co^{2+} and Cu^{2+} onto zeolites ZSM-5, HY, and 4A, *J. Environ. Chem. Eng.*, 2021, **9**, 106126.